UNIVERSITÀ DEGLI STUDI DI MILANO

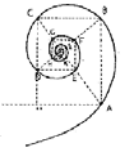

DOTTORATO IN MEDICINA MOLECOLARE E TRASLAZIONALE

CICLO XXX

Anno Accademico 2016/2017

TESI DI DOTTORATO DI RICERCA
Settore Scientifico Disciplinare MED/26

A NEW PROCEDURE TO ISOLATE BRAIN MITOCHONDRIA FROM HUMAN CORTEX AND ITS APPLICATION FOR LIPID ANALYSIS IN PHYSIOLOGICAL AGING

Dottoranda: Alice VALMADRE
Matricola N°R10848

TUTORE: Prof.ssa Stefania Paola CORTI
CO-TUTORE: Dott. Luigi ZECCA

COORDINATORE DEL DOTTORATO: Ch.mo Prof. Riccardo GHIDONI

"Non esistono condizioni ideali in cui scrivere, studiare, lavorare o riflettere, ma è solo la volontà, la passione e la testardaggine a spingere un uomo a perseguire il proprio progetto."
Konrad Lorenz (1903-1989), scienziato austriaco.

"There are no ideal conditions to write, study, work or think, rather, it is just will, passion and stubbornness that push a man to pursue his own project".
Konrad Lorenz (1903-1989), Austrian scientist.

Sommario

Molti studi hanno rivelato l'importanza dei mitocondri come organelli cellulari significativamente coinvolti nell'insorgenza o nella progressione di malattie neurodegenerative, il cui principale fattore di rischio è l'invecchiamento. I protocolli attuali per l'isolamento dei mitocondri cerebrali sono stati sviluppati per preservarne la vitalità, sacrificando la purezza necessaria per eseguire analisi biochimiche ad alta prestazione. Il mio progetto di dottorato si è concentrato sullo sviluppo di una nuova procedura, al fine di ottenere una frazione mitocondriale altamente purificata, a partire da tessuti congelati post-mortem di corteccia cerebrale umana di soggetti sani. La valutazione dell'arricchimento mitocondriale e di altri contaminanti cellulari è stata eseguita attraverso diversi saggi enzimatici, analisi di western blot e microscopia elettronica a trasmissione. Questi esperimenti di convalida hanno dimostrato la purezza dei mitocondri e la loro integrità, nonché la conservazione delle membrane associate ai mitocondri. Il processo di invecchiamento cerebrale è ritenuto responsabile della modifica chimica di lipidi e di cambiamenti nella composizione lipidica delle membrane cellulari. In questo contesto, non esistono studi precedenti sui lipidi di mitocondri cerebrali umani. Pertanto, questo nuovo metodo è stato applicato per studiare la composizione lipidica di mitocondri puri mediante cromatografia su strato sottile. Inoltre, abbiamo indagato se ci fossero cambiamenti correlati all'invecchiamento nella composizione lipidica in questi organelli essenziali alla vita e alla morte cellulari, in quanto ciò potrebbe portare a una riduzione della funzionalità della membrana mitocondriale stessa.

Abstract

Many studies have revealed the importance of mitochondria as cellular organelles decisively involved in the onset or progression of neurodegenerative diseases, whose main risk factor is aging. Current protocols for brain mitochondria isolation have been developed to preserve viability, sacrificing the purity that is required to perform high-throughput biochemical analyses. My Phd project focused on the development of a new procedure to obtain a highly pure mitochondrial fraction starting from post mortem frozen tissues of human brain cortex of healthy subjects. The evaluation of mitochondrial enrichment and other cellular contaminants has been performed through different enzyme assays, western blot analyses and transmission electron microscopy. These validation experiments demonstrated the purity of mitochondria and their integrity, as well as the preservation of mitochondria-associated membranes. The brain aging process is allegedly responsible for chemical modification of lipids and changes in the lipid composition of cell membranes. In this scenario, there are no previous studies on human brain mitochondria lipids. Thus, this new method has been applied to investigate lipid composition of pure mitochondria by means of thin layer chromatography. Furthermore, we investigated if there were aging related changes in the lipid composition of these organelles essentials to cell life and death, since that could produce an impairment of the membrane function.

Index

Abbreviations

List of the abbreviations used in the text, in order of appearance.

VDAC = voltage-dependent anion channel

ADP = adenosine diphosphate

ATP = adenosine triphosphate

MPTP = mitochondrial permeability transition pore

CoQ/Q = coenzyme Q

Cyt c = cytochrome c

ANT = adenine nucleotide translocator

ROS = reactive oxygen species

RNS = reactive nitrogen species

MnSOD = mitochondrial superoxide dismutase

CL = cardiolipin

AAC = ADP/ATP carrier

PINK1 = PTEN-induced kinase 1

PD = Parkinson’s disease

AD = Alzheimer’s disease

Aβ = amyloid beta

LRRK2 = leucine-rich repeat kinase

PE = ethanolamine glycerophospholipids

PC = choline glycerophospholipids

PI = inositol glycerophospholipids

PG = glycerol glycerophospholipids

PA = phosphatidic acid

SL = sphingolipids

SM = sphingomyelin

PAF = platelet activating factor

C1P = ceramide-1-phosphate

S1P = sphingosine-1-phosphate

GPI = glycosylphosphatidylinositol-anchored proteins

TM = transmembrane proteins

Acyl = dually acylated proteins

MAG = myelin-associated glycoprotein

TOM = translocase of the outer membrane

SAM = sorting and assembly machinery

TOM-22 = translocase of the outer membrane 22 homolog

BSA = bovine serum albumin

EGTA = ethylene glycol tetraacetic acid

PIC = protease inhibitor cocktail

EDTA = ethylenediaminetetraacetic acid

GalCer = galactosylceramide

GlcCer = glucosylceramide

LacCer = lactosylceramide

MIB = mitochondria isolation buffer

OD = optiprep diluent

HMF = heavy mitochondrial fraction

CS = citrate synthase

LDH = lactate dehydrogenase

AP = acid phosphatase

CAT = catalase

PDI = disulfide isomerase

TLC/HPTLC = thin layer chromatography/ high-performance TLC

BH = brain homogenate

MAM = mitochondria-associated membranes

MF = mitochondrial fraction

2D-TLC = two dimensional TLC

1. Introduction

1.1 The origin of mitochondria

The discovery of mitochondria occurred in the middle of the nineteenth century and, although it derived from the contributions of several scientists, it should be attributed to the former who has detected mitochondria, the Swiss anatomist and physiologist Rudolf Albert von Kölliker, who described granular structures in muscle tissue cells [1]. These structures were then better described by the German pathologist Richard Altmann, who observed particular granules in almost all cellular types and called them “bioblasts” (life germ) (Fig.1).

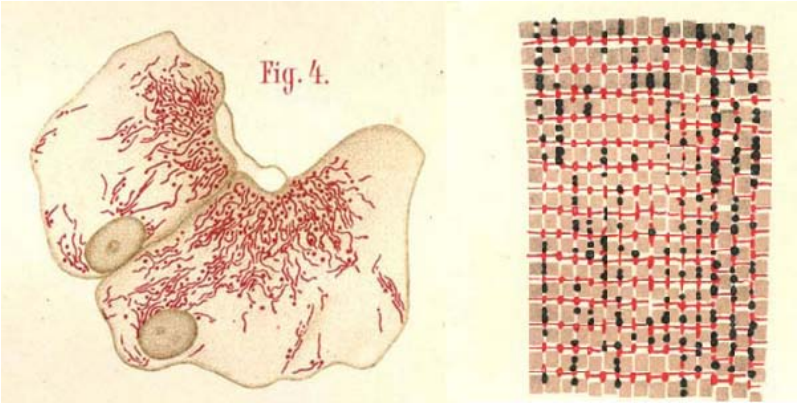

Figure 1. Histological drawings of “bioblasts” in flight muscle (right) and liver cells (left) as described by Altmann [2].

Altmann explained in his book that these “bioblasts” were elementary organisms with genetic and metabolic autonomy, suggesting that they could have been symbionts as well as the fundamental units of cellular activity [2]. Unfortunately, Altmann's theories were not accepted by his colleagues, although in the 1960s the American scientist Lynn Margulis Sagan would have resumed his speculations by suggesting that mitochondria derived from certain bacteria endocyted by host cells, becoming endosymbionts [3].

Eight years later, thanks to the microscope, the microbiologist Carl Benda noticed particular bodies during insect spermatogenesis in both filamentous and granular form, so he gave them the current name mitochondrion, referring to the appearance of these organelles [4]. Indeed, the etiology of the word “mitochondrion” comes from the fusion of two terms in ancient Greek: the words “μῖτος” (mitos) meaning thread and “χόνδρος” (chondros) meaning granule.

1.2 The morphology and structure of mitochondria

In the 20th century, the knowledge about mitochondria increased exponentially due to the advancement of biochemical, genetic and instrumental techniques, such as the use of electron microscopy. What do we know now about these intriguing organelles? They are present in the cytoplasm of all aerobic eukaryotic cells and have a spherical or elongated shape that is nearly the size of a bacterium, being correlated both from a structural and an evolutionary point of view [5].

Mitochondria have a diameter of about 0.5 μm and a length of about 1-2μm, but they can reach a size up to 10 μm in length. Their number can vary from only one mitochondrion in some unicellular algae to tens of thousands in oocytes but, in

most cases, they are on average 500-1000. Their shape and volume may be modified due to osmotic and chemical changes, in fact, mitochondria swell and contract after metabolic processes or in relation to changes of osmotic pressure in the cellular environment [6]. Although the external form of mitochondria is variable, their internal structural organization is highly conserved [7].

Mitochondria move freely in the cytoplasm and tend to thicken where the demand for energy is greater (i.e, in fibers muscles surrounding myofibrils or in synapses of nervous system). The movement of mitochondria has been recognized as a result of intricate interactions between proteins on the outer surface and various components of the cytoskeleton, which include actin filaments, microtubules, and intermediate filaments [8]. With the advent of the electron microscope it was possible to study the ultrastructural organization of mitochondria. It is delimited by a double membrane: an external membrane in contact with the cytoplasm and an internal membrane that folds over many times and creates layered structures called “cristae”. Both membranes have a thickness of about 5-6 nm and delimit a volume of about 8-20 nm called compartment or intermembrane space. The internal membrane encloses the mitochondrial matrix (Fig. 2).

The outer membrane is smooth and rather elastic, has a relatively simple constitution, with about 50% of lipids and 50% of proteins and with reduced transport functions. Its structure is very similar to that of plasma membrane and other cellular compartments but, a unlike these, it has a great permeability [9, 10]. Indeed, mitochondria contain the voltage-dependent anion channel (VDAC) (also known as mitochondrial porin), which polymerizes and forms pores (aqueous transmembrane channels) in the mitochondrial outer membrane, making it freely

permeable to ions and molecules with a molecular weight of less than 5000 Dalton [11]. Such permeability is confirmed by the biochemical composition of intermembrane space, which is similar to that of cytoplasm.

The inner membrane is structurally and functionally much more complex than the outer membrane. Approximately 80 % consists of proteins and the remaining 20 % of lipids [9]. The inner membrane differs from all other cellular membrane systems for the absence of cholesterol in its lipid skeleton and for having a high content of cardiolipin [12], an acidic phospholipid. Moreover, the inner membrane contains most of the enzymes involved in the transport of electrons and oxidative phosphorylation, various dehydrogenases and different transport systems that catalyze the transfer of substrates, metabolic intermediates and adenyl nucleotides between the cytosol and the matrix [9].

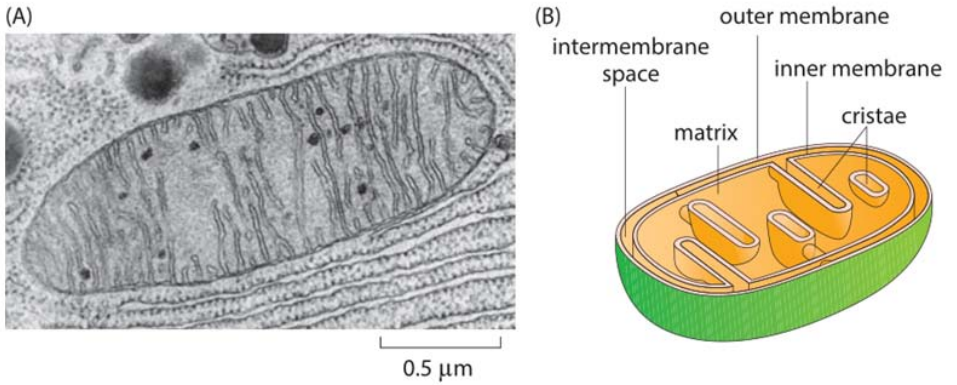

Figure 2. Ultrastructural mitochondrial organization. A) Electron micrograph. B) Schematic representation (Source: http://book.bionumbers.org/how-big-are-mitochondria/)

Little is known about the intermembrane space, but electron microscopy demonstrated the presence of contact sites between membranes, thus forming contiguous zones between the outer and inner membranes [13]. This space also contains proteins, such as cytochrome, that play major roles in mitochondrial energetic metabolism and apoptosis [14].

The matrix is a gel-like material that contains ribosomes, most of the enzymes that are responsible for the citric acid cycle reactions and the enzymes involved in fatty acid oxidation. Through electron tomography of neuronal mitochondria Perkins and colleagues found out that a specific subdomain of the inner membrane called “cristae membrane” form invaginations that protrude into matrix space through narrow, tubular openings they called “cristae junctions” [15] (Figure 3). The attachments of cristae to the inner boundary membrane is not described as infoldings but as small tubes with the diameter of 30 nm [16]. This new information about the mitochondrial structure can have important functional implications: it is assumed that "cristae junctions" can be a barrier to the free diffusion of ions and metabolites like ADP (adenosine diphosphate) between the intercristal and intermembrane spaces [16]. Moreover, inside the matrix, there are several copies of the mitochondrial chromosome.

The human mitochondrial DNA (mtDNA) is relatively small (16569 bp), circular, double-stranded and contains 37 genes coding for two rRNAs, 22 tRNAs and 13 polypeptides, which are all subunits of enzyme complexes of the oxidative phosphorylation system [17]. The other proteins required for the respiratory chain are coded by nuclear DNA, which implies a close complementation between the

two genetic systems. The mtDNA is transmitted through maternal line, since mitochondria are almost exclusively inherited by the zygote from the oocyte [18].

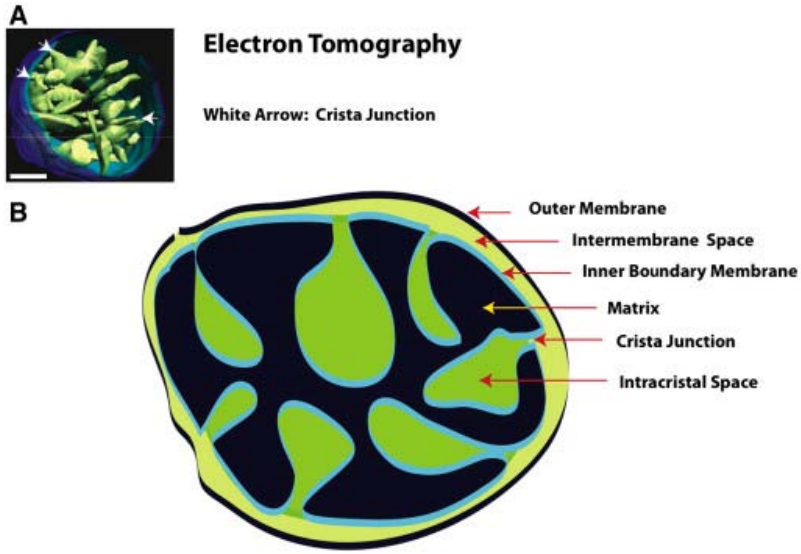

Figure 3. Model of mitochondria based on EM tomography. Mitochondria have three distinct compartments separated by two membrane systems. The inner membrane consists of two parts, the cristae membranes and the inner boundary membrane. These junctions have been proposed to regulate the dynamic distribution of proteins, lipids, and metabolites between mitochondrial compartments. A) A surface-rendered view of an isolated liver mitochondrion generated from an electron tomographic volume. Scale = 100 nm. (B) A model of the crista junction in relation to mitochondrial compartments. Reproduced by Yamaguchi *et al*. 2009 [19].

1.3 Endosymbiosis hypothesis

About 1.5 billion years ago the very first nucleated cell appeared on the earth. Lynn Margulis Sagan proposed that, during the transition to the oxidizing atmosphere, eukaryotes originated from the survival of a heterotrophic anaerobe that ingested an aerobic prokaryotic microbe [3]. As stated above, this is supported by many existing analogies between mitochondria and bacteria. They have similar size and both have one single circular chromosome, which retains genes encoding rRNAs, tRNAs, proteins involved in redox reactions, and proteins required for transcription, translation, and replication [17]. Respiratory chain enzymes are present in the membrane of bacteria and in the mitochondrial internal membrane. In addition, the bacterial membrane has introflexions (mesosomes) similar to mitochondrial cristae. Like bacteria, mitochondria have no histones and their ribosomes are sensitive to certain antibiotics such as chloramphenicol [20]. Moreover, mitochondria are formed only through binary fission, the form of cell division used by bacteria and archaea [21]. Transport proteins called porins are found in the outer membranes of mitochondria and as well as in bacterial cell membranes [22]. Cardiolipin is found only in the inner mitochondrial membrane and bacterial cell membranes [23]. From all these circumstances, it has been hypothesized that the inner membrane and the mitochondrial matrix represent the symbiont which was originally enveloped by the plasma membrane and embedded in the eukaryotic cell.

1.4 Mitochondrial Functions

Mitochondria are involved in many and important cellular processes (Table 1) and in particular they play the fundamental function of recovering the energy contained in the foods, converting it into chemical energy in the form of ATP (adenosine triphosphate). As a matter of fact, despite differing in structure and function in different cells, mitochondria are always "closed spaces" where most of the energy metabolism takes place [24]. Among scientific milestones, the early studies on cell respiration and oxidative phosphorylation were performed by Battelli and Stern, who studied biological oxidation [25], and by Warburg who reported that respiration was linked to particles [26], later called “grana”, involved in strengthening of “respiratory enzymes” [27]. In 1948, Eugene Kennedy and Albert Lehninger identified mitochondria as the cell compartment where oxidative phosphorylation occurs [28]: this process satisfies about 90 % of the energetic need of cells, through the reoxidation of reduced pyridinic and flavinic coenzyme (NADH and $FADH_2$ respectively), catalyzed by the redox complexes of respiratory chain leading to ATP synthesis.

Mitochondria functions include other essential metabolic pathways, such as the citric acid cycle, fatty acid oxidation, the synthesis and degradation of aminoacids (urea cycle), and the synthesis of iron–sulfur clusters and heme. Mitochondria can work as temporary calcium deposits considering their ability to store it rapidly; this contributes to the overall homeostasis of this ion, which is involved in various cellular reactions such as signal transduction. Calcium is imported into the matrix through a uniport driven by the membrane potential on the inner membrane and released through Na^+/Ca^{2+} transporter or a Ca^{2+}-induced release pathway [29, 30].

Mitochondria therefore function as an intracellular calcium reserve along with the endoplasmic reticulum, with which there is close communication [31].

Location/Product(s)	Function(s)
All Cells and Tissues	Oxidative phosphorylation
All Cells and Tissues	Apoptosis (programmed cell death)
Tissue or Cell-specific	Cholesterol metabolism
Tissue or Cell-specific	Amino and organic acid metabolism
Tissue or Cell-specific	Fatty acid beta oxidation
Tissue or Cell-specific	Sex steroid synthesis
Tissue or Cell-specific	Heme synthesis
Tissue or Cell-specific	Hepatic ammonia detoxification
Tissue or Cell-specific	Neurotransmitter metabolism
Tissue or Cell-specific (new)	Regulating cell division
Tissue or Cell-specific (new)	Controlling calcium supply
Non-coding RNAs (new)	Controlling genetic code expression
Humanin peptide (new)	Protection against Alzheimer, diabetic, arterial plaques

Table 1. Functions of mitochondria (Source: https://universe-review.ca/F11-monocell11a.htm)

Moreover, mitochondria are of cardinal relevance not only in maintaining cellular life but also in controlling programmed cell death (apoptosis) through complex mechanisms that can culminate with the opening of the mitochondrial permeability transition pore (MPTP), that it is a transmembrane channel voltage-dependent, belonging to the inner membrane. Its irreversible opening causes uncoupling of the respiratory chain with loss of the electrochemical gradient, cessation of ATP

synthesis, release of mitochondrial proteins from intermembrane space (i.e., cytochrome c, Smac / Diablo and AIF), and Ca^{2+} outflow from the matrix [32]. Many of these events favor in turn the opening of the pore causing the amplification of the process. The final result is a massive osmotic swelling of the mitochondria with subsequent mitochondrial membrane rupture and complete depolarization.

1.4.1 Fusion and fission

Mitochondrial fusion and fission processes are closely related to major events in the apoptosis process. Indeed, in most cell types, mitochondria are organized within a network of organelles, but at the beginning of the apoptotic process the network tends to fragment [33]. The term mitochondrial fission means the breakdown of the mitochondrial network in small isolated organelles. It is a typical process that manifests during cell division in order to assure the inheritance of the mtDNA. This process also occurs during differentiation in response to changes in the cell energy need or to toxic stress. Mitochondrial fission is essential for providing the growing and dividing cells with an adequate number of mitochondria. The mitochondrial fusion process is needed to maintain the network of mitochondria and for the correct functioning of these organelles. Indeed, a network densely interconnected, can mitigate the effects of environmental damage through the exchange of proteins and lipids with other mitochondria. The fusion-fission cycle is therefore a balance of two concurrent processes: one redeems the damage, while the other eliminates it [34].

1.4.2 The electron transport chain

Through the electron transport chain, the mitochondria fulfill the ATP cell demand by performing oxidative phosphorylation. This process consists of a series of electron transporters (complexes), most of which are embedded in the inner membrane, containing prosthetic groups able to accept and donate one or two electrons. The electron transporters complexes originally described are four; Complex I, Complex II, Complex III and Complex IV. Additionally, two moving electron carriers are needed: coenzyme Q (CoQ or Q) and cytochrome c (Cyt c).

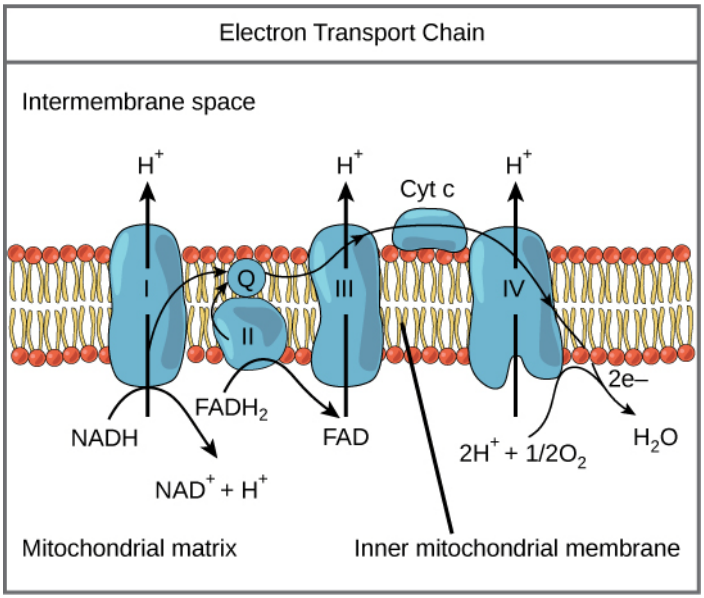

Figure 5. Representation of complexes embedded in the inner membrane with electron flow leading to O_2 and production of ATP. (Source: https://www.boundless.com/biology/textbooks/boundless-biology-textbook/cellular-respiration-7/oxidative-phosphorylation-76/electron-transport-chain-362-11588/)

Our knowledge on ATP synthesis is mainly based on the hypothesis proposed by Peter Mitchell in 1961, in which energy translation occurs through the creation of transmembrane protonic gradients associated with electronic transfer: the chemiosmotic theory [28]. The outer membrane is permeable, in contrast to the internal one, even against small molecules and almost all ions including protons (H^+); the only chemical species that can cross the membrane are those that possess a specific transporter inserted into the membrane itself. These are the key features for the creation and maintenance of the protonic gradient. The respiratory chain receives electrons coming from different pathways by reducing equivalents (NADH and $FADH_2$). Electrons derived from NADH are transferred to Complex I and then to CoQ, while those derived from succinate are transferred to $FADH_2$ and then to Complex II, hence to CoQ. From CoQ the electrons pass to Complex III, to Cyt c, then to Complex IV and finally to molecular oxygen to give H_2O (Figure 5). The free energy released by the electron flow is coupled to the endoergonic transport of protons through the inner mitochondrial membrane. This proton transport produces both a chemical gradient (ΔpH) and an electrical gradient ($\Delta\Psi$), generating a protonic electromotive force that drives the protons from the intermembrane space to the matrix; as the inner membrane is impermeable to the protons, these, in order to return, must pass through the specific domain F_0 of the transmembrane channel called ATP synthase (or Complex V). The driving force that pushes the protons into the matrix provides the energy required for ATP synthesis, catalyzed by the F_1 domain of ATP synthase. Part of the ATP is used for the mitochondrial needs, but the majority is transported out of the organelle through the adeninucleotide transporter (ANT) and used for different cellular functions.

1.4.3 Reactive oxygen species (ROS)

Mitochondria are considered the largest source of reactive oxygen species (ROS) [35] whose production is inevitable during normal oxidative metabolism and increases considerably in pathological conditions [36]. Oxygen is a highly oxidizing molecule, so it easily accepts electrons from other molecules, producing partially reduced products, known as ROS. Since these species have one or more free electrons (free radicals), they are unstable and particularly reactive, so they tend to pair the electrons by yielding or receiving an opposite spin electron from other molecules, to achieve a stable conformation. These partially reduced species can react with other radicals, but also with non-radical organic molecules such as carbohydrates, nucleic acids, lipids and proteins, generating a series of chain reactions damaging biological systems [37].

The ROS include superoxide anion ($O_2^{\cdot -}$) and its radical conjugated acid ($HO_2^{\cdot}$); the hydroxyl radical ($OH^{\cdot}$), carbonate ($CO_3^{\cdot -}$), peroxyl ($RO_2^{\cdot}$) and alkoxyl ($RO^{\cdot}$). Even some neutral, non-radical species are considered ROS, among them hydrogen peroxide (H_2O_2), HOCl, reactive aldehydes, singlet oxygen and lipid hydroperoxides (LOOH) [38,39]. Similarly, reactive nitrogen species (RNS) includes both radical species such as nitrogen monoxide ($NO^{\cdot}$) and non-radical species, such as nitrous acid (HNO_2), nitrosyl cation (NO^+), nitroxyl anion (NO^-), dinitrogen trioxide (N_2O_3), dinitrogen tetraoxide (N_2O_4), nitronium (nitryl) cation (NO_2^+), organic peroxides (ROOH), aldehydes (HCOR) and peroxynitrite (ONOOH) [40].

Increased concentration of ROS and reactive nitrogen species (RNS) causes "oxidative stress". This phenomenon is the result of a disequilibrium in the homeostasis of reactive species: in normal cells, excess ROS or RNS is prevented by scavenging systems and by the ability of some of these species (H_2O_2) to permeate the mitochondrial membrane freely in cytosol, where they play physiological roles and are detoxified [41].

The mitochondrial respiratory chain is the main source of reactive oxygen species in a cell, particularly superoxide anion. Mitochondrial $O_2^{\bullet -}$ production takes place at redox-active prosthetic groups within proteins, or when electron carriers such as reduced-CoQ are bound to proteins. The kinetic factors favor or prevent the one-electron reduction of O_2 to $O_2^{\bullet -}$, that determine mitochondrial $O_2^{\bullet -}$ production [42]. $O_2^{\bullet -}$ released into the matrix is detoxified by a specific superoxide intramitochondrial dismutase (MnSOD), which catalyzes the following reaction: $2\ O_2^{\bullet -} + 2H^+ = O_2 + H_2O_2$. Then, the reduction of H_2O_2, is performed by the enzyme glutathione peroxidase, responsible for most detoxification of intracellular hydrogen peroxide; the reaction needs glutathione, whose deficiency is associated to mitochondrial dysfunction and consequent cell damage [43].

1.4 Cardiolipin

Cardiolipin (CL) is the signature phospholipid of the mitochondria and has a pleiotropic function inside the organelle. Its primary function is associated with ATP production along with the electron transport chain, suggesting a fundamental role in the bioenergetic process. CL interacts with several inner membrane proteins and enzymes, acting as a co-factor for optimal activity [44]. Among these, all the

electron transport chain complexes and ADP/ATP carrier (AAC) have shown to be tightly bound to CL molecules [45-53]. The AAC allows the ATP to pass across the inner membrane to intermembrane space, after oxidative phosphorilation. Claypool asserted that, although it is unknown how CL facilitates normal AAC physiology, the high affinity between AAC and CL is strongly implicated in full AAC function [54]. Indeed, Imai and colleagues showed that, in rat brain mitochondria, AAC activity requires either CL or phosphatidylglycerol [55]. Alike, CL binding to Complex I, or Cytochrome c oxidase, stabilizes all subunits interactions to regulate the electron activity of the enzyme [56] and its binding to Complex III is required for the enzyme maintenance and stability, as well as its functional and structural integrity [57].

Furthermore, CL is involved in apoptosis process through the interaction with Cyt c; CL bound to Cyc c and act as a peroxidase, catalyzing CL peroxidation which is required for release of Cyt c during apoptosis [58]. It must be underlined that CL is a phospholipid easily susceptible to ROS attack because particularly rich in unsaturated fatty acids and because of its location in the inner membrane, near to the site of ROS generation [59]. For these reasons, it is easy to perceive how oxidative damage may have deleterious effects on mitochondrial function. Moreover, Petrosillo and colleagues showed that exogenous added oxidized CL sensitized isolated mitochondria to Ca^{2+}-induced MPTP opening and release of cytochrome c [60], and also oxidation of endogenous CL resulted in MPTP opening [61].

1.5 The role of mitochondria in brain aging

In the central nervous system, the importance of mitochondrial bioenergy lies in the fact that neurons require high ATP consumption to perform their functions. The loss of the complex dynamic balance of the mitochondria is an alarm bell for cellular damage and can drive to cell death. Brain energy metabolism declines with age [62], and mitochondria can be involved in cellular mechanisms that can be impaired both in physiological and pathological aging, such as chronic neurodegenerative diseases of the senile brain [63]. It is well known that brain synapses are the core components of the central nervous system: they allow a signal (electrical or chemical) to pass from one neuron to another. Mitochondria are concentrated in presynaptic terminals by active transport to provide energy supply for information transfer [64]. Despite the well documented plasticity of the synaptic junction areas, these peculiar zones of the neuronal membrane undergo serious deteriorative events during aging. Indeed, Bertoni-Freddari and co-workers carried out a morphometric study on the ultrastructural features of synaptic mitochondria in cerebellar glomeruli of adult and old patients, and found a significant impairment in the mitochondrial dynamic morphology [65].

1.5.1 The “mitochondrial theory of aging”

In 1956 the biogerontologist Denham Harman published a theory, known as the “free radical theory of aging”, based on the belief that damage by ROS is critical in determining life span [66]. When the free radical theory of aging is focused on mitochondria, it emerges as the “mitochondrial theory of aging” [67]. As mitochondria continue to generate ROS throughout the cell life, a chronic oxidative

stress is produced and this phenomenon increases oxidation of mitochondrial proteins, lipids and DNA. ROS also inhibits aconitase activity and thereby affects the tricarboxylic acid cycle [68]. A proteomic analysis in rat cerebellum showed an increased protein nitration during aging [69]. The MnSOD activity is inhibited by nitration and, not surprisingly, it decreases linearly in aged mice brain mitochondria [70]. This means that, inside mitochondria, a powerful antioxidant defense is overwhelmed during aging. Moreover, it should be stressed that the brain is highly vulnerable to oxidative damage because of a relative lack of anti-oxidant enzymes, an abundance of oxidizable substrates like polyunsaturated fatty acids, catecholamines, a high content of redox-active transition metals in certain brain regions and a high rate of oxygen utilization per gram weight of tissue [71,72].

1.5.2 Oxidative phosphorylation and aging

Aging can damage oxidative phosphorylation through various mechanisms. For example, decreasing the enzymatic activity of one of the electron transport chain complexes can slow the oxidative phosphorylation rate. However, the maximum enzymatic activity expressed by the complexes of the electron transport chain seems to be in excess respect to phosphorylation, so that a 30-50% decrease in its activity is necessary to achieve a real reduction in the maximum phosphorylation speed [73]. However, disparate experimental systems have shown an impairment of electron transfer complexes in old rat brains [74,75] and in old mice brains [76,77].

1.5.3 Mutations of the mitochondrial genome

The accumulation of somatic mtDNA mutations and the subsequent cytoplasmic segregation of these mutations have been shown to contribute to aging process in human brain areas such as putamen and cortex [78]. Besides, it has been demonstrated that brain mtDNA from elderly individuals had a higher aggregate of mutations than brain mtDNA from younger individuals. The average aggregate mutational burden in elderly subjects was $2 \times 10^{(-4)}$ mutations/bp [79]. The mutation $mtDNA^{4977}$ is a 4,977 bp deletion of the mitochondrial genome usually found in patients with Kearns-Sayre disease, a genetic mitochondrial myopathy. Through PCR analysis, Soong and co-workers measured in 12 brain regions of 6 normal adults (humans) the levels of $mtDNA^{4977}$ and presented interesting data: a comparison of the same region between subjects showed an increase of $mtDNA^{4977}$ with age. Particularly, the highest levels were in regions characterized by a high dopamine metabolism: caudate, putamen and substantia nigra, while cerebellum showed no age-related increase [80]. A possible explanation of the elevated rate of mutations observed in the mtDNA (much higher than for nuclear DNA) may be explained by the fact that mtDNA is highly exposed to ROS: 1) it is located very near the inner mitochondrial membrane where ROS are produced, 2) it is not excessively condensed or protected by histones and 3) it has limited repair activity.

1.5.4 Mitophagy

In order to maintain a proper cellular bioenergetic status, several quality control mechanisms are implemented to eliminate damaged or misfolded mitochondrial proteins [81]. Malfunctioning organelles can accumulate through aging, and so it is

important to entirely degrade damaged mitochondria. In this case, the cell activates a mechanism called mitophagy, which is a selective form of macroautophagy, fundamental for cellular homeostasis and implicated in several disease [82].

Various papers have showed that the depolarization of the mitochondrial membrane leads to stabilization of PINK1 (PTEN-induced kinase 1), that in turn recruits the E3 ubiquitin ligase Parkin to mitochondria which can trigger mitophagy [83-85] (Figure 6). Since the PINK1-parkin pathway is known to be involved in the hereditary form of Parkinson's disease [86], alterations in mitophagy machinery may be linked to aging and age-related diseases [87]. Although the details of this process need to be further investigated, it seems that the regulation of mitophagy shares primary steps with the macroautophagy pathway, while displaying different regulatory steps specific for mitochondrial autophagic turnover [89].

Nutrient starvation is a well-established mechanism of increased longevity among species because it activates autophagy by inhibiting the Insulin/PI3K/TOR signalling pathway [90]. The removal of damaged mitochondria through mitophagy could be one of the contributing factors of increased life span by caloric restriction. Moreover, it has been reported that low levels of ROS act as signal for mitophagy [91]. For example, Kirkland and colleagues found that nerve growth factor (NGF)-deprived rat sympathetic neurons revealed cardiolipin loss and mitochondrial mass decline together with increased production of ROS species and increased lipid peroxidation. They were able to block peroxidation, loss of cardiolipin, and the decrease of mitochondrial mass with the use of antioxidant agents. So they suggested that this decline, caused by autophagy of damaged mitochondria, derived

from augmentation of ROS production [92]. On the other side, high ROS levels mediate p53 activation that induces autophagy inhibition [93] and exhibits prooxidative activities that further increase the stress level, leading to cell death [94].

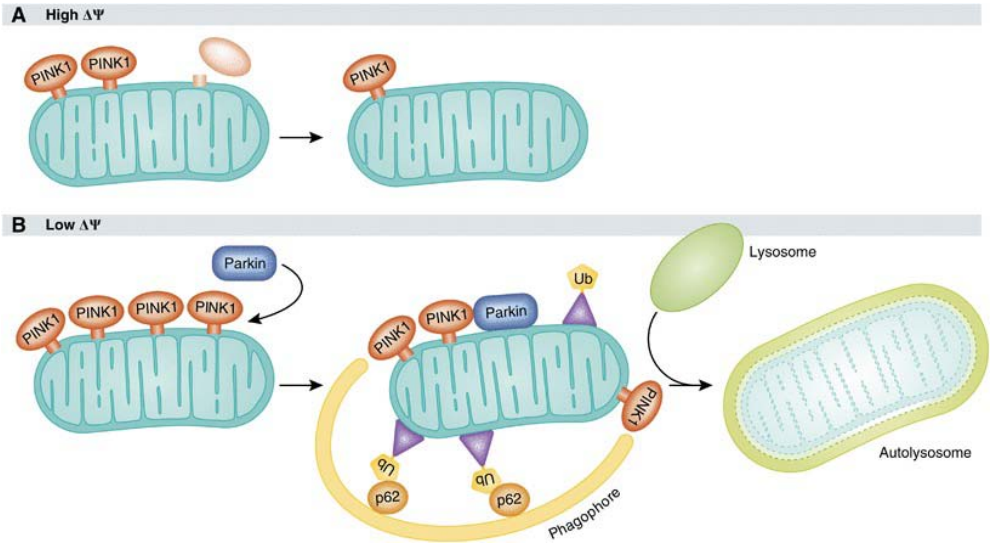

Figure 6. Mechanism of PINK1 and parkin-induced mitophagy. (A) If the mitochondrial membrane potential is high, PINK1 is imported into mitochondria, proteolytically processed and rapidly degraded. (B) If mitochondria are depolarized, PINK1 accumulates on the mitochondrial surface, recruits parkin, which ubiquitinates mitochondrial proteins. This process is followed by the recruitment of the adaptor protein (p62), which link ubiquitinated cargo to the autophagic machinery. The organelle is engulfed by phagophore, which mature into autophagosome, fuse with lysosome to form autolysosome, and finally digest its content by mitophagy. Reproduced from Exner *et al.* 2012 [88].

1.6 Mitochondria and age-related diseases

It is interesting to note that brain mitochondrial dysfunctions and oxidative stress have a pivotal role in the pathogenesis of both Parkinson's Disease (PD) and Alzheimer's Disease (AD), although the molecular link between these age-related diseases and the physiological brain aging is still obscure [95].

1.6.1 Mitochondria involvement in Alzheimer's Disease

AD is the most common form of degenerative dementia and begins predominantly in the senile age permanently affecting many cognitive faculties [96]. As the average life expectancy progressively increases, the proportion of patients affected continuously heightens, becoming a priority for public health. There are currently no preventive therapies, but only therapeutic interventions to mitigate the symptoms. Many factors contribute to the difficulty of the study approach: the lack of information on the pathophysiology of the disease, the lack of an animal model to study the pathological processes and evaluate the efficacy of therapies, and the absence of a definite biomarker for early stage diagnosis [97].

At histological level AD brain shows a strong protein accumulation: β-amyloid peptide (Aβ) is the major component of the extracellular neuritic plaques, while hyperphosphorylated tau protein is the major component of intracellular neurofibrillary tangles. The molecular events leading to the development of sporadic late-onset AD have not been settled. As aging is the greatest risk factor for AD, and energy metabolism is reduced, it has been proposed that mitochondrial dysfunction could be the primary event that causes Aβ deposition, synaptic degeneration, and formation of neurofibrillary tangles [98,99]. In fact, Bubber and

coworkers found in AD brains a significant decrease in the activities of three TCA cycle enzymes: pyruvate dehydrogenase complex, isocitrate dehydrogenase and alpha-ketoglutarate dehydrogenase complex [100]. Moreover, there is also a diminished activity of COX in platelets and hippocampus from AD patients compared to controls [101] and an impairment of mitochondrial biogenesis thus suggesting and involvement of mitochondrial abnormalities during the disease [102].

1.6.2 Mitochondria involvement in Parkinson's disease

After AD, PD is the most common neurodegenerative disorder in individuals over the age of 65. The most common symptoms of the disease are: "resting tremor, plastic rigidity, paucity or delayed initiation of movement, slowness and impaired postural and righting reflexes" [103]. The fundamental macroscopic anatomopathological alteration in PD brain is the loss of pigmented neurons in the pars compacta of the substantia nigra with the microscopic presence of inclusion bodies called "Lewy bodies" in surviving neurons [104]. PD and parkinsonism become clinically appreciated only when about 50-70% of dopaminergic cells is lost [105]. This cell loss results in reduced dopaminergic projection to putamen and therefore a dysfunction of the basal ganglia [106].

In the last few decades, mitochondrial dysfunction has been strongly associated with PD: indeed, complex I activity was reported to be significantly reduced in mitochondria of substantia nigra [107] and in frontal cortex from post mortem brain of PD subjects [108]. Besides, Bender and colleagues showed how levels of deleted mtDNA were higher in dopaminergic neurons from PD patients in

comparison to age-matched controls [109]. Since complex I is considered one of the major producer of ROS [110], it is not surprising that dopaminergic neurons, which are exposed to a high oxidative burden, are particularly vulnerable to mtDNA damages. Looking at familial PD, there are several mutated genes linked to mitochondria. PINK 1 and parkin, both described above for their fundamental role in mitophagy, are associated with autosomal recessive PD [111,112]. Additionally, mutations in the DJ-1 gene, encoding a protein whose function is still largely unknown, is associated with early onset autosomal recessive PD [113]. There is some demonstration that DJ-1 might play a role in preventing cell death as antioxidant defense [114], and that its loss leads to reduced mitochondrial membrane potential [115]. Furthermore, Irrcher and coworkers reported that DJ-1 deficient cultured neurons, mouse brain and lymphoblast cells derived from patients displayed aberrant mitochondrial morphology, which is a sign of perturbation of their dynamic [116]. Finally, mutations in leucine-rich repeat kinase 2 (LRRK2) gene remain the most common cause of late onset autosomal dominant familial PD and some case of sporadic PD [117]. LRRK2 is present mainly in cytoplasm, but is also linked to outer mitochondrial membrane, similar to the localization of Parkin. In PD, the critical feature of LRRK2 is its enhanced kinase activity, so it might be a target of therapeutic intervention [118].

1.7 Human brain lipids

1.7.1 Lipid composition of human brain

The primary biological functions of lipids in the body are the following: deposit of chemical energy in storage fat (triglycerides), and structural constituents of cell membranes. Lipids are the most common biomolecules present in the brain (12 %) and account for 50 % of its dry weight [119], suggesting an elemental role. The lipid composition of the whole human brain is chiefly formed by: 1) phospholipids which include ethanolamine glycerophospholipids (PE), serine glycerophospholipids (PS), choline glycerophospholipids (PC), inositol glycerophospholipids (PI), glycerol glycerophospholipids (PG), phosphatidic acid (PA); 2) sphingolipids (SL), which includes sphingomyelin (SM), ceramide and glycolipids (i.e. gangliosides, galactocerebrosides); 3) cholesterol and free fatty acids [120]. Table 2 reports the lipid composition of normal human brain tissue, displaying differences between gray and white matter (table 2).

The various glycerophospholipid species, along with cholesterol and sphingolipids, represent the greatest components of cell membranes generating the structure and fluidity of somatodendritic and axonal membranes of neurons, and also of those of the glia and other cell types, as well as various intracellular organelles [121]. Glycerophospholipids are a family of amphipathic molecules distributed asymmetrically across the plasma membrane and are composed by a polar head group with a glycerol backbone and a phosphobase (ethanolamine, inositol, choline, etc.), and a non-polar tail group consisting of two fatty acid chains [122]. As all membrane possess a typical composition with more or less the same classes

of glycerophospholipids, the ratio between these classes and their molecular species are unique and provide membranes from different cellular organelles with specific characteristics [123].

Sphingolipids are amphipatic membrane lipids, which share the same double tailed hydrophobic moiety, ceramide, responsible for their insertion in the glycerolipid bilayer of biological membranes [124].

Lipid	Gray matter	White matter
Cholesterol	19.6	26.9
Phosphatidylethanolamine	30.7	19.6
Phosphatidylcholine	25.1	11.8
Galactocerebroside	7.2	18.4
Phosphatidylserine	7.2	9.0
Phosphatidylinositol	3.9	4.0
Sphingomyelin	3.2	4.4
Sulfatid	0.7	5.1
Phosphatidic acid	0.5	0.4
Unidentified	1.9	0.4
Sum	100	100

Table 2. Percentages of total lipid composition distinguished in white and gray matter of human brain tissue. Gangliosides could belong to the unidentified species. Reproduced from Krafft *et al.* 2005 [125].

Ceramide is composed by a long-chain amino alcohol, known as sphingosine, linked via an amide bond with a variable length fatty acid chain. The term “sphingosine” is also used to identify uncommon structures with shorter and longer

alkyl chain [126]. Sphingomyelin belongs to the group of sphingophospholipids. It is composed of a ceramide backbone with a PC residue attached.

Among glycosphingolipids, the hydrophilic moiety is represented by an oligosaccharide chain, whose structure can range from a very simple one, such as galactose in galactosylceramide, to a higher degree of complexity such as sialic acids (sugar residues containing a carboxyl group) in gangliosides. Due to their highly hydrophilic and bulky saccharidic head group, gangliosides have a strong polar character and they are present at elevated levels in neurons [127]. Since they are heterogeneous molecules, both in the oligosaccharide and ceramide portions, gangliosides are classified according to the oligosaccharide sequence and the number of sialic acid residues bound to it by an α-glycosidic bond. In the Svennerholm classification for brain gangliosides, letter G denotes ganglioside, letter M is a mono-sialic acid residue, D is for di- , T for tri- , and Q indicates tetrasyalic acid phosphingolipids [128,129]. A number is then assigned to the individual compound, which was initially referred, to its migration into a particular chromatographic system.

Cholesterol is a lipid with a unique structure consisting of four linked hydrocarbon rings forming the bulky steroid structure. There is a hydrocarbon tail linked to one end of the steroid and a hydroxyl group linked to the other end. The hydroxyl group is able to form hydrogen bonds with nearby carbonyl oxygen of glycerophospholipid and sphingolipid head groups.

1.7.2 Lipids functions in human brain

Neurochemists initially thought that the absence of triglycerides in the brain meant that lipids had only a mere structural function in the central nervous system. Subsequent studies revealed that non-membrane lipids are also bioactive compounds (i.e. steroid hormones and eicosanoids) and, later, that membrane lipids, which were previously believed to have only a structural role, also have crucial functions in signal transduction across biological membranes [130].

1.7.2.1 Glycerophospholipids

In neural membranes, several glycerophospholipids influence the fluidity, permeability, balance of hydrophilic and hydrophobic membrane components, charge, reactivity to regulate membrane-bound enzyme activity and ion-channels [131,132]. Moreover, glycerophospholipids have other crucial functions in brain metabolism as second messenger reservoir. After phospholipase stimulation by different agonist, such as hormones or neurotransmitter, an intricate signalling cascade activates different metabolic pathways. For example, phospholipase A_2 produces arachidonate, eicosanoids and platelet activating factor (PAF) starting from PC, PE and PI, while phospolipase C produces diacylglycerol and IP3 starting from PI [133]. PAF has many important roles in brain tissue: it is a retrograde messenger in memory formation [134], activates protein kinase c, modulates the levels of neuropeptides and regulates neuronal differentiation [135].

Glycerophospholipids that contain alk-1-enyl groups are called plasmalogens and are major components of the phospholipids of the mammalian brain [136]. Plasmalogens may function like a natural antioxidant because their vinyl ether

linkages display reactivity with ROS [137] and may be involved in membrane fusion during synaptic transmission thanks to the higher capacity of PE plasmalogens to form non-lamellar lipid structures [138].

1.7.2.2 Sphingolipids and cholesterol

Ceramide is a cell membrane component involved in the neobiosynthesis and catabolism of both sphingomyelin and glycosphingolipids [139](Fig. 7). Ceramides and other intermediates of sphingolipid metabolism are key players in intracellular signaling and are involved in apoptosis, cell senescence, proliferation, cell growth and differentiation [140]. The biosynthetic pathway of sphingolipids first leads to ceramide, which generates sphingomyelin and glycosphingolipids. The processing of these molecules can produce a range of bioactive lipid species which includes ceramide-1-phosphate (C1P), ceramide, sphingosine and sphingosine-1-phosphate (S1P) [141]. S1P is essential for development of the brain [142], calcium homeostasis [143], cellular growth [144], inhibition of apoptosis [145, 146], histone modifications [147], and nuclear factor-κB signalling [148]. While S1P and C1P have antiapoptotic effects and favour cell survival, the corrispectives sphingosine and ceramide are proapoptotic and associated with growth arrest [149, 150].

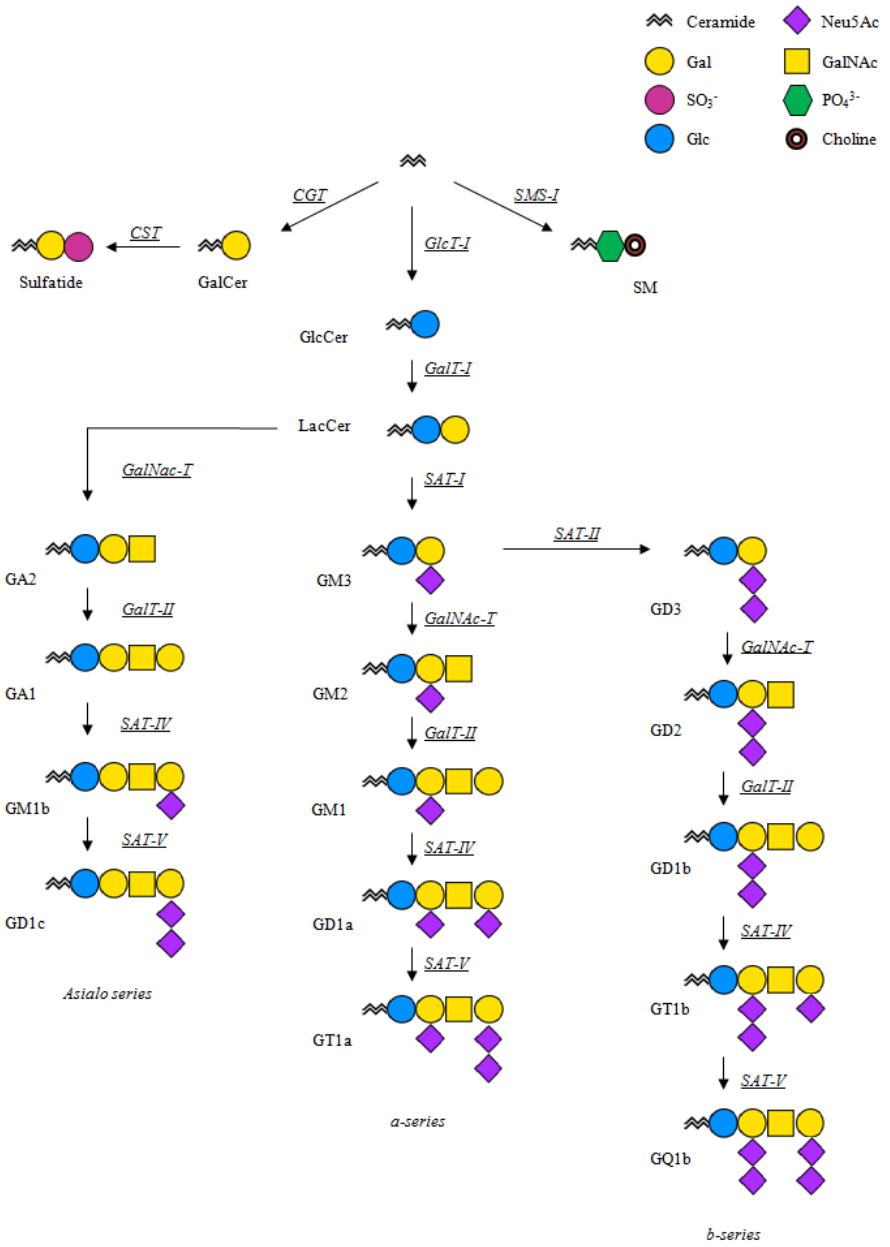

Figure 7. Schematic biosynthetic pathway of glycosphingolipids.

Within the membrane ocean there are lipid structures of elevated cholesterol and glycosphingolipid content named “lipid rafts” [151] (Fig. 8). Lipid rafts incorporate also different proteins involved in various aspects of nervous system function: a variety of receptor systems, such as G protein-coupled receptors [152] and neurotransmitter receptors [153, 154]. Acting as signaling platforms, lipid rafts are involved in many events in the development and maintenance of neuronal functions, as well as in the interactions between neurons and glial cells [155]. In addition to provide correct membrane fluidity and permeability, cholesterol and sphingolipids can interact with acetylcholine and serotonin receptors through typical binding sites located in both their transmembrane helices and the extracellular loops. Therefore, these lipids regulate neurotransmitter binding and signal transducing functions by altering the conformation of the receptors [156].

Furthermore, slight variation in membrane cholesterol content can dramatically impair the function of nearby proteins [157]. The dysregulation of cholesterol metabolism in the brain has been linked to age-associated neurodegenerative disorders such as AD. It has been recently reviewed that microRNAs (miRNAs) are implicated as novel regulators of cholesterol metabolism in several tissues: indeed, ABCA1, an important membrane-associated lipid pump that plays a key role in maintaining cholesterol homeostasis, is negatively regulated by miR106b [158]. Kim and colleagues have shown that miR-106b significantly decreased ABCA1 levels and impaired cellular cholesterol efflux resulting in increasing Aβ production and preventing Aβ clearance in neuronal cells [159]. The interaction between SM and cholesterol has many important functions within cell compartments, such as the recruitment of integral protein to the lipid bilayer and the involvement in caveolae formation during endocytosis [160].

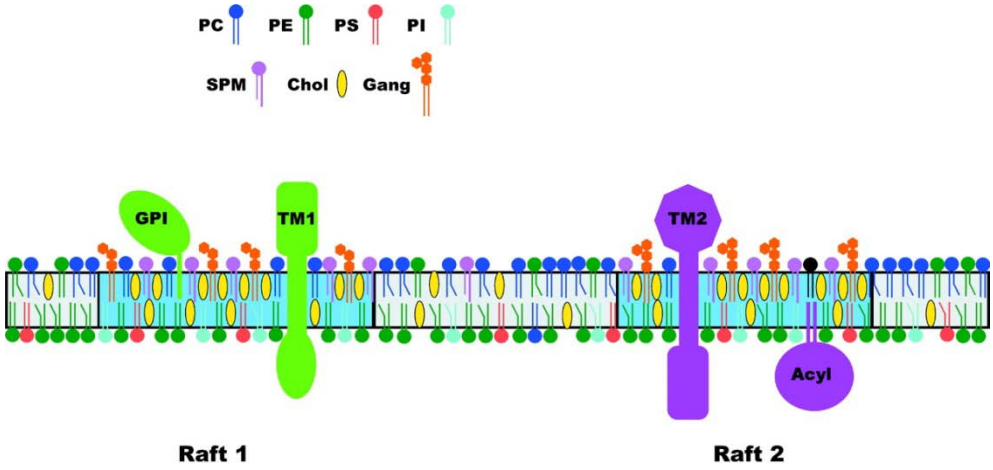

Figure 8. Schematic structure of plasma membrane (white bilayer) with lipid rafts (blue bilayer). This composition results in lateral phase separation and the generation of a liquid-ordered domain. Cholesterol, sphingomyelin, and gangliosides, are enriched in lipid rafts. As shown, Raft 1 and Raft 2 differ in protein and lipid composition. Glycosylphosphatidylinositol-anchored proteins (GPI); transmembrane proteins (TM); dually acylated proteins (Acyl). Reproduced from Pike 2003 [151].

1.7.2.3 Gangliosides

Gangliosides play a key role in the formation and stabilization of specific cell lipid membrane domains (glycolipids-rich domains) through their oligosaccaridic moieties protruding on the outer membrane surface. Acting as modulators of cell recognition, signaling and adhesion, gangliosides are considered functional molecules of biological relevance [161]. They also have been indicated to be present in nuclear membranes, where GM1 modulates intracellular and intranuclear calcium homeostasis and the ensuing cellular functions [162].

An involvement of gangliosides during brain development underline an additional tissue-specific task: indeed, the ganglioside pattern sustains a decisive changing during neural growth. At the beginning there is a predominance of GD3 and GM3, while later in the development there is an increase in more complex gangliosides such as GM1, GD1a, GD1b and GT1b [163].

Glycosphingolipids are also known to play a role in the regulation of axonal growth. For example, gangliosides GD1a and GT1b, enriched in axonal rafts, act as myelin-associated glycoprotein (MAG) receptors in MAG-induced inhibition of axonal growth [164].

1.8 Lipids of mitochondria

Each cellular organelle has its own distinctive membrane lipid composition, that produces a characteristic structure, shape and specific functions [165]. As the mitochondria possesses two biochemically different membranes, the complexity of their lipid composition can influence structure and morphology. Furthermore, it has been reported that mitochondrial membrane lipids support different mitochondrial enzyme activities such as voltage-dependent ion channel and respiratory chain complexes [166, 167]. The stability of TOM (translocase of the outer membrane) and SAM (sorting and assembly machinery) complexes requires the dimeric form of CL to correctly import and assembly α-elical and β-barrel proteins, while PE maintains the function of TOM only for the biogenesis of β-barrel proteins [168].

Kiebish and co-workers recently examined the mouse brain mitochondrial lipidome through mass spectrometry. As shown in table 3, the main lipid species represented in mitochondria are PE, PC and cholesterol. Next, the signature lipid of mitochondria CL, which is enriched in the inner membrane, followed by glycerophospholipid minor classes PI, PG, SM, PS, LysoPC and ceramide in traces [169].

Lipid	Non-synaptic	Synaptic
Ethanolamine glycerophospholipids	187.4 ± 12.1	211.7 ± 21.3
Phosphatidylethanolamine	164.9 ± 10.0	184.6 ± 20.3
Plasmenylethanolamine	22.5 ± 2.2	27.0 ± 1.0
Choline glycerophospholipids	129.9 ± 7.7	156.3 ± 26.1
Phosphatidylcholine	119.6 ± 5.3	137.4 ± 17.2
Plasmenylcholine	1.2 ± 0.1	2.4 ± 1.1
Plasmanylcholine	9.1 ± 3.2	16.5 ± 8.5
Cholesterol	139.0 ± 46.7	126.7 ± 31.2
Cardiolipin	52.7 ± 4.5	39.9 ± 3.4 *
Phosphatidylinositol	9.4 ± 0.8	10.2 ± 0.9
Phosphatidylglycerol	7.1 ± 0.5	6.4 ± 0.7
Sphingomyelin	5.3 ± 1.2	6.5 ± 0.6
Phosphatidylserine	4.6 ± 1.5	14.1 ± 3.0 *
Lysophosphatidylcholine	2.7 ± 0.6	3.3 ± 0.4
Ceramide	0.7 ± 0.2	1.6 ± 0.2 **

Values are expressed as mean nmol/mg protein ± S.D. (N = 3)

Significantly different values from NS mitochondria at

*: $P < 0.02$;

**: $P < 0.005$ as determined from the two-tailed *t*-test

Table 3. Lipid composition of C57BL/6J mouse brain mitochondria. Reproduced from Kiebish *et al.* 2009 [169].

1.9 First steps toward mitochondria isolation

The first attempt of subcellular fractionation to isolate mitochondria has to be attributed to the Nobel Prize Albert Claude, who was engaged from the late 1930s in this detailed study [170] basing on the previous procedure of Bensley and Hoerr [171]. His contributions introduced the differential centrifugation as fundamental tissue fractionation technique [172], as well as the study of chemical composition and biochemical activities of the obtained fractions. Moreover, he was the first scientist who establish the importance of using an homogenization isotonic medium, that would prevent osmotic changes potentially damaging the organelle morphology. Claude's procedure provided four fractions: a heavy fraction of nuclei and cell debris, an intermediate fraction consisting of mitochondria, a light fraction containing "microsomes" (endoplasmic reticulum fragments) and a soluble cytosolic fraction [173]. Few years later, Hogeboom, Schneider, and Palade [174] modified Claude's procedure by replacing the isotonic salt solution used as homogenization medium with a hypertonic (0.88 M) sucrose solution. This substitution eliminated aggregation of the different particles, improving the purity of the fractions and the quality of the isolated mitochondria. The homogenization medium was further modified [175] by employing isotonic (0.25 M) rather than hypertonic sucrose improving the sedimentation of different fractions and also avoiding the inhibitory effect of high concentrations of sucrose on certain enzymes. This procedure became the routine method for preparing mitochondria. Many steps forward have been made since then, in fact the protocols have been developed and diversified depending on the specific properties of tissue or cell types involved and its successive application.

1.9.1. Isolation of mitochondria from brain samples

Nowadays there are numerous methods for the isolation of mitochondria from brain tissue, based on gentle cell breakage, differential centrifugation and disparate density gradients [176-184]. Most of these procedures utilize a rapid isolation of mitochondria for enzymatic studies, sacrificing their purity for viability required for functional (respiration) based studies. On the contrary, the emergence of high-throughput "omics" technologies demanded an optimization of purity, because other contaminants, even in scarce amounts, would affect results of the analyses. Therefore, equilibrium centrifugation in density gradients is the preferred technique to separate mitochondria from other cell components. The principle on which it is based on concerns the differences in densities of single organelles, influenced substantially by their different ratios of protein to lipid species. Mitochondrial inner membranes consist of 70–80 % of protein and hence tend to have a higher density than, for instance, endosomal membranes, which have higher lipid content. The most widely used medium for density gradient centrifugation of proteins is sucrose, but Percoll^{tm} (a colloidal suspension of tiny silica particles coated with polyvinylpyrrolidone or PVP) is more frequently used for the isolation of brain mitochondria. Indeed, mitochondria from mammalian brain tissues were routinely prepared for proteomics by density gradient centrifugation using Percoll [185, 186]. Finally, there is also a relatively new approach used to isolate functional mitochondria from brain tissue, that is based on superparamagnetic microbeads conjugated to anti-TOM22 (translocase of outer mitochondrial membrane 22 homolog) antibody, which specifically bind to mitochondria outer membrane [187, 188].

2. Aim of the study

Mitochondria are the main energy providers of the cell. Many studies have demonstrated the importance of mitochondria as cellular organelles decisively involved in brain aging mechanisms. Moreover mitochondrial membrane lipids do not only have a structural role, but also sustain different mitochondrial enzyme activities such as voltage-dependent ion channel and respiratory chain complexes. For these reasons, the aim of the project is the investigation of the lipid composition of human brain mitochondria and its changes in physiological aging. Since information about lipid composition of human brain mitochondria are extremely poor, a full characterization needs to be performed first. Furthermore, in order to obtain reliable data, mitochondria must be highly purified. Current protocols for brain mitochondria isolation are more developed to preserve viability at the expense of the purity that is required by detailed biochemical techniques and, commonly, they are optimized on mouse or rat brain tissues. To our knowledge, protocols for isolation of human brain mitochondria have been developed modifying Sims and Anderson isolation protocol of rat brain mitochondria. The preliminary step of this study was the application of this method to isolate mitochondria from post mortem human frontal cortex: since results did not fulfill requirements, the first aim of this study was to develop a new satisfying method to obtain a highly purified mitochondrial fraction. For this purpose, validating biochemical assays such as enzymatic assays had to be defined to assess mitochondria purity and integrity, in addition to information obtained by transmission electron microscopy. Furthermore, this newly developed method was applied for the analysis of mitochondria lipid molecular species and for the

investigation of their age-related changes, thus providing a basis for better understanding of their role in this physiological process.

3. Materials and methods

3.1. Materials

3.1.1. Human samples

Brain samples were obtained during autopsies of male (n=5) and female (n=2) subjects (average age 58 years old) who died without evidence of neuropsychiatric and neurodegenerative disorders. Informed consents for using brain samples for research purposes were obtained from closest relatives and are stored at the Section of Legal Medicine and Insurances, Department of Human Biomedical Sciences for Health, University of Milan. Final approval was given by the pathologist executing the autopsy. Samples of premotor (frontal) cortex were carefully dissected into white and grey matter and then stored at -80°C until use for the isolation of mitochondria. All tissues samples were analyzed anonymously.

3.1.2 Materials

Sucrose, d-Mannitol, Hepes, Tris(hydroxymethyl)aminomethane, Optiprep^{tm}, Bovine serum albumin (BSA), Ethylene glycol-bis(2-aminoethylether)-N,N,N′,N′-tetraacetic acid (EGTA), Protease Inhibitor Cocktail (PIC), all reagents to set up enzyme assay reactions and solvent systems for thin layer chromatography were purchased from *Sigma-Aldrich Co*. Sodium Hydroxide and Ethylenediaminetetraacetic acid disodium (EDTA) were purchased from *Carlo Erba Reagents*. Pure galactosylceramide (GalCer), sulfatides, and lyso PC were purchased from *Avanti Polar Lipids*; phosphatidylcholine (PC), phosphatidylethanolamine (PE), phosphatidylinositol (PI), phosphatidylserine (PS),

sphingomyelin (SM), and phosphatidic acid (PA) were purchased from *Sigma-Aldrich Co*. Ceramide, gangliosides (GM3, GM2, GM1, GD3, GD1a, GD1b, GT1b, GQ1b), glucosylceramide (GlcCer), and lactosylceramide (LacCer) were synthesized or purified in Prof. Prinetti laboratories (Department of Medical Biotechnology and Translational Medicine, University of Milan, Segrate Milano, Italy).

3.1.3. Equipment

Potter-Elvehjem PTFE pestle and glass tube (Sigma-Aldrich Co.). Benchtop refrigerated high speed centrifuge Thermo Scientific MR23i with swinging bucket rotor (SWM 180.5) and angle fixed rotor (AM 100.13). Ultracentrifuge Optima XE-90 (Beckman Coulter) with swinging bucket rotor (SW41Ti Beckman Coulter). Centrifuge tubes: 15-ml glass round bottom tubes (Corning cod. 8441), 10/11-ml polystyrene conical bottom tubes (Nunc cod. 347856), 13.2-ml Ultra-Clear tubes^{tm} (Beckman Coulter cod. 344059). Laboratory filters for liquids (Euroclone) with vacuum pump. Plastic Petri dishes 60x15mm (Greiner cod.628161). Disposable plastic and glass Pasteur pipettes. Adjustable volumetric pipettes: 20µl, 200µl and 1ml total volume.

3.2. Methods

3.2.1. Reagent setup

- Mitochondria Isolation Buffer (MIB): 75 mM sucrose, 225 mM d-mannitol, 1 mM EGTA, 1 mM EDTA, 5 mM HEPES, pH 7.40 in ultra-pure water. The pH was adjusted to 7.4 with NaOH. The solution was then filtered and stored at -20°C for up to 3 months.
- Optiprep^{tm} Diluent (OD): 250mM sucrose, 2mM EGTA, 2mM EDTA, 35mM Hepes, pH 7.4 in ultra-pure water. The pH was adjusted to 7.4 with NaOH. The solution was then filtered and stored at -20°C for up to 3 months.
- Optiprep^{tm} Diluent 2 (OD2): 75 mM sucrose, 225 mM d-mannitol, 1 mM EGTA, 1 mM EDTA, 20 mM HEPES, pH 7.40 in ultra-pure water. The pH was adjusted to 7.4 with NaOH. The solution was then filtered and stored at -20°C for up to 3 months.
- 20% (vol/vol) Optiprep^{tm} solution: 2 ml of OD2 were mixed with 1 ml of 60% Optiprep^{tm} solution. This solution was freshly prepared and stored on ice.
- 30% (vol/vol) Optiprep^{tm} solution: 1.5 ml of OD2 was mixed with 1.5 ml of 60% Optiprep^{tm} solution. This solution was freshly prepared and stored on ice.

3.2.2 Isolation Protocol

Mitochondria were isolated from frozen post-mortem human prefrontal cortex. We used exclusively grey matter from premotor cortex since it contains more cell bodies, while white matter contains almost exclusively fibers. All equipment and

reagents were placed on ice and all the centrifuge steps were executed at 4°C. Figure 9 shows a schematic diagram of all the protocol steps.

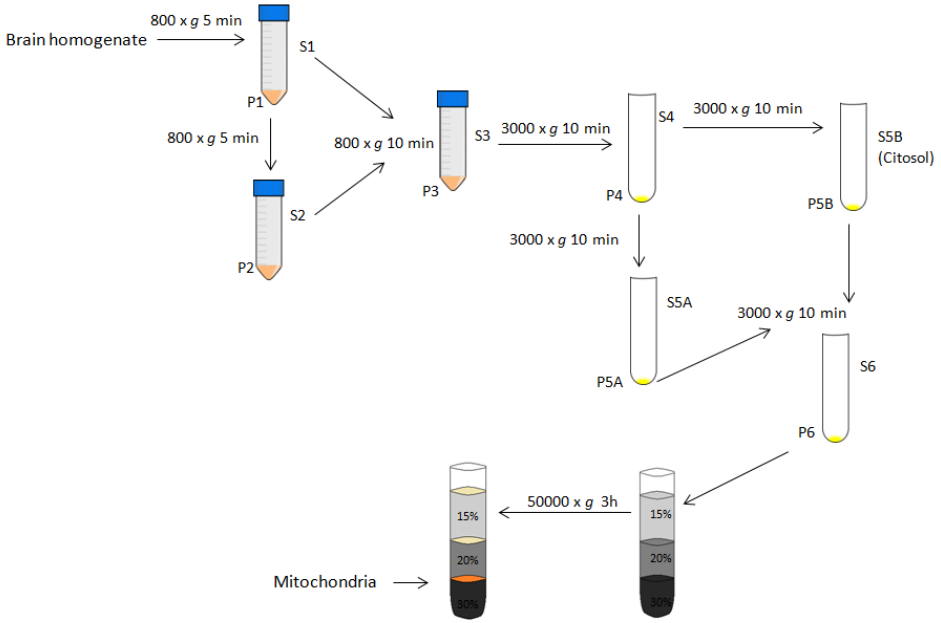

Figure 9: Diagram of the mitochondria isolation protocol. For explanation see description in the text.

3.2.2.1. Preparation of crude heavy mitochondrial fraction (HMF)

The preparation of the crude fraction containing heavy mitochondria is schematically described as follows.

- A solution containing 1mg/ml of BSA and 1% (v/v) of PIC was added to MIB only before use.

- The brain tissue (1g of wet weight tissue) was placed in a small Petri dish.
- The tissue was transferred into the glass potter and 2 ml of MIB were added.
- The tissue was gently homogenized using 13 up-and-down strokes of a glass/Teflon pestle while rotating it.
- The homogenate was placed in a 10-ml conical bottom centrifuge tube and 5 ml of MIB were added. The tube was gently mixed by inversion.
- A sample of 100 µl was collected for subsequent evaluation of total tissue enzymes or proteins.
- The homogenate was centrifuged at 800 x g at 4°C for 5 min using a swinging-bucket rotor (SWM 180.5). The supernatant (S1) was withdrawn, without collecting the pellet (P1), and retained on ice.
- 2 ml of MIB were added to the tube and the pellet (P1) was gently resuspended with a plastic Pasteur pipette.
- The suspension was poured in the pestle and homogenized again with 6 slow up-and-down strokes. The homogenate was transferred in a new tube and fresh 4 ml of MIB were added.
- The homogenate was centrifuge again at 800 x g at 4°C for 5 min using a swinging-bucket rotor (SWM 180.5), the supernatant (S2) was withdrawn by suction, without transferring the pellet (P2), and pooled with S1.
- The pooled supernatants (S1+S2) were centrifuged at 800 x g at 4°C for 10 min using a swinging-bucket rotor (SWM 180.5). The small pellet (P3) formed was the proof that it was necessary to further remove contaminants.

- The supernatant (S3) was then collected and centrifuged in a round bottom glass tube at 3000 x g at 4°C for 10 min using a fixed angle rotor (AM 100.13).
- The supernatant (S4) was transferred into a new tube (B) and the mitochondrial pellet (P4) gently resuspended with 1 ml of MIB. Then, 5 ml of MIB were added and the suspension poured in a different tube (A).
- Both tubes were centrifuged at 3000 x g at 4°C for 10 min using a fixed angle rotor (AM 100.13).
- From tube B the supernatant (S5B) was collected and stored separately. The pellet (P5B) was resuspended with 1 ml of MIB. From tube A the supernatant (S5A) was discarded and the pellet (P5A) resuspended with 1ml of MIB. Then, P5A and P5B were pooled.
- About 4 ml of MIB were added to the suspension, which was then centrifuged at 3000 x g at 4°C for 10 min using a fixed angle rotor (AM 100.13).
- The supernatant (S6) was discarded and the pellet (P6) resuspended with 1ml of OD.

3.2.2.2 Fractionation of crude HMF

The fractionation of the crude HMF obtained is schematically described as follows.

- In a Ultra-clear centrifuge tube (14x89 mm) 3 ml of 30% Optiprep^{tm} solution were layered with a glass Pasteur pipette; 3 ml of 20% Optiprep^{tm} solution were slowly layered above the 30% Optiprep^{tm} keeping the tube at

45° and loading the sample by directing the flow onto the wall near the surface of the liquid. This procedure generated a sharp interface between the 30 % layer and the 20 %.

- To produce a 15 % solution, 2 ml of OD and 1 ml of Optiprep^{tm} 60 % were added to the sample. The suspension was gently layer with a glass Pasteur pipette on the discontinuous gradient, as described before. The tube was then filled with 1 ml of OD.
- The tube was centrifuged at 50.000 x g (Sw 41Ti rotor) at 4°C for 3 hours using slow acceleration and deceleration. This centrifugation redistributed the material into three major bands (Fig. 10).
- The material accumulated on the top of the gradient was removed with a plastic Pasteur pipette (Band 1 in Fig. 8), and the pale band at the interface between 15% and 20% (Band 2 in Fig. 8) was removed with a glass Pasteur pipette.
- The mitochondrial fraction at the interface between 20% and 30% (Band 3 in Fig. 8) was removed with a glass Pasteur pipette and poured in a 15 ml glass round bottom tube. Then, 5 ml of MIB (without PIC and BSA) were added, gently resuspending the mitochondrial fraction with a plastic Pasteur pipette.
- The tube was centrifuge at 3000 x g at 4°C for 10 min using a fixed angle rotor (AM 100.13).
- The supernatant was discarded and the pellet collected by resuspending it with 90µl of MIB.

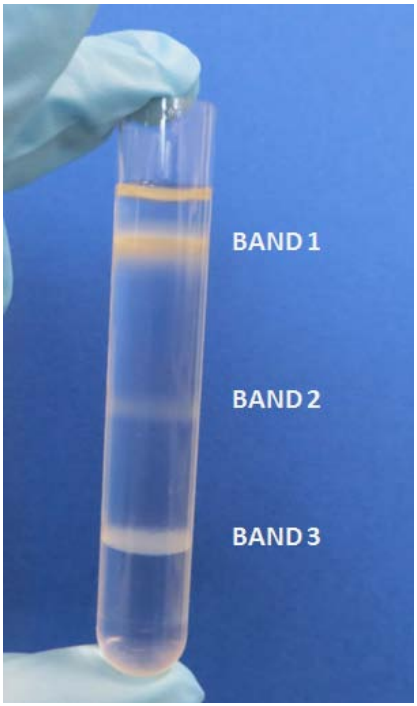

Figure 10: The image shows the typical appearance of a centrifuge tube at the end of the density gradient ultracentrifugation step. Purified mitochondria are located in band 3.

3.2.3 Enzyme assays

The activity of all maker enzymes was assayed in the initial homogenate and the final mitochondrial fraction. In order to measure mitochondrial enrichment, citrate synthase (CS) activity was measured immediately after the isolation procedure, adjusting the conditions reported by Morgunov and Srere [189]. The purity of the obtained fraction was evaluated assaying the activity of different enzymatic markers, as explained hereafter. Lactate dehydrogenase (LDH), as cytosolic marker, was estimated in both of these fractions; in fact, LDH provides a measure of the contamination by synaptosomes in which cytoplasm is enclosed within a membrane. The assay was performed using LDH activity assay kit from *Sigma-Aldrich Co.* Moreover, to assess lysosomal and peroxisomal contamination, acid phosphatase (AP) activity and catalase (CAT) activity were quantified in the same previous fractions through AP assay kit and CAT assay kit respectively, both from *Sigma-Aldrich Co*. The activities were determined using spectrophotometric techniques. The quantification of proteins was carried out after protein precipitation, through Lowry's method [190], using BSA as protein standard.

3.2.4 Western blotting

Aliquots of isolated mitochondria and brain homogenates were subjected to freeze-thaw cycles and sonication. Equal amounts of proteins were heated in reducing sample buffer [191] and then loaded onto 1.50 mm thick polyacrylamide mini gels (12%) and separated by one-dimensional sodium dodecyl sulfate-polyacrylamide gel electrophoresis (Mini-PROTEAN® 3 Cell; Bio-Rad Laboratories, Inc., Hercules, CA, USA). Prestained protein markers (*New England BioLabs Inc.*,

Ipswich, MA, USA) were used as size standards in the electrophoresis. Proteins were transferred at 350mA for 3 hours (*Mini Trans-Blot® Electrophoretic Transfer Cell; Bio-Rad Laboratories, Inc*.) to 0.45 µm nitrocellulose membranes (*Amersham Hybond®-ECL; GE Healthcare Life Science*). Ponceau-S staining of membranes was performed to check the efficiency of proteins transfer. For immunoblotting, membranes were blocked for 2 hours at room temperature with 5% fatty acid/globulin-free bovine serum albumin (*Sigma-Aldrich Co*.) or 5% skimmed milk, depending on the antibody, in phosphate-buffered saline (pH 7.4) with 0.1 % *Tween*® 20 (PBST). Then membranes were incubated overnight at 4°C in the primary antibody with PBST. The primary antibodies used to evaluate protein expression are:

- Disulfide Isomerase (PDI) at 1:1000 (*Cell Signaling*);
- Histone H3 at 1:2000 (*Cell Signaling*);
- GRP75 at1:1000 (*Cell Signaling*);
- PYK2 at 1:1000 (*Bd Transduction*);
- Paxillin at 1:1000 (*Bd Transduction*).

After overnight incubation in primary antibody, the membranes were rinsed three times in PBST and incubated in secondary antibody for one hour r.t. in HRP-conjugated goat anti-rabbit IgG (1:5000) or anti-mouse IgG (1:3000). The blots were rinsed thoroughly in PBST and were developed using *Pierce SuperSignal West Pico chemiluminescent substrate* and then exposed to CL-XPosure film (*Thermo Scientific*).

3.2.5 Total lipid extraction, phase partitioning and alkali treatment

Lipids from the lyophilized samples were extracted with chloroform/methanol/water 20:10:1 (v/v/v) and subjected to a modified two-phase Folch's partitioning to obtain the aqueous and the organic phases [192]. Briefly, 1240 μL of the solvent system were added to the lyophilized samples. The samples were then mixed, incubated at r.t. for 15 minutes and centrifuged at 16100 g, and finally kept at r.t. for 15 minutes. The supernatant was collected as total lipid extract and the extraction was repeated again twice by adding the 1550 μL of the solvent system to the pellets. The pellets were air dried and resuspended in 1N NaOH and incubated overnight at r.t. before being brought to 0.05N NaOH with water to allow the determination of the protein content with DC assay (*Bio-Rad*). Aliquots of the total lipid extract were then subjected to phase partitioning adding 20 % of water by volume. The samples were then mixed, incubated at r.t. for 15 minutes and centrifuged at 16100 g, and finally kept at r.t. for 15 minutes. The aqueous phase were recovered, and chloroform:water 1:1 (v/v) were added to the organic phase before mixing the samples, incubated at r.t. for 15 minutes, centrifuged at 16100 g, and finally kept at r.t. for 15 minutes. The new aqueous phases were recovered and united to the ones previously collected. The aqueous phases were dried under N_2 flux, and resuspended in water before undergoing microdialysis and lyophilization. The organic phases were dried under N_2 flux and resupended in a known volume of chloroform/methanol 2:1. Aliquots of the organic phases were then subjected to alkali treatment to remove glycerophospholipids [192].

3.2.6 Thin layer chromatography (TLC)

To determine endogenous lipid content, the various samples were analyzed by monodimensional silica gel high performance TLC using different solvent systems. The total lipid extracts were analyzed using chloroform/methanol/0.2% calcium chloride 60:35:8 (v/v/v) as a solvent system, the aqueous phases were analyzed with chloroform/methanol/0.2% calcium chloride 50:42:11 (v/v/v), whereas the organic phases and the methanolyzed organic phases were analyzed using chloroform/methanol/water 110:40:6 (v/v/v). The organic phases were also analyzed by two-dimensional HPTLC using two different solvent systems: chloroform/methanol/water 14:6:1 (v/v/v) for the first separation and chloroform/methanol/acetic acid 13:5:2 (v/v/v) for the second separation. The cholesterol quantitation was performed using hexane/ethylacetate 3:2 (v/v), whereas detection of ceramide was executed with hexane/chloroform/acetone/acetic acid 20:70:20:4 (v/v/v/v). After separation, lipids were detected either by spraying the TLC plates with different colorimetric reagents (anisaldehyde, aniline, Ehrlich's reagent and phospholipids-reactive) or by TLC immunostaining. Identification of lipids after separation and chemical detection was assessed by co-migration with lipid standards.

3.2.7 TLC immunostaining

Gangliosides were detected by TLC-immunostaining with cholera toxin after sialidase treatment. Samples were spotted on a silica gel TLC plate and developed in chloroform/methanol/0.2 % calcium chloride (50:42:11, v/v). After evaporation of the solvent at room temperature, the plate was dipped three times with a

polyisobuthylmethacrylate solution, and air dried for 1 hour before being immersed in blocking solution (1 % BSA in 0.1M Tris-HCl pH 8, 0.14M NaCl) for 30 minutes. The plates were then incubated with 0.12 U/mL sialidase (*Sigma-Aldrich Co*) in 0.05 M acetate buffer, pH 5.4, containing 4mM $CaCl_2$, at r.t. overnight. Thereafter the plates were overlaid with cholera toxin B subunit-HRP conjugated (1:200, *Sigma-Aldrich Co*) in phosphate-buffered saline with 1% bovine serum albumin at r.t. for 1 h. After few washes, plates were developed using o-phenylenediamine (OPD)/H_2O_2 in 0.05 M citrate-phosphate buffer pH 5.0.

3.2.8 Electron microscopy

Pellets containing mitochondria were fixed for 2 hours in a mixture of 4 % paraformaldehyde and 2 % glutaraldehyde in cacodylate buffer (0.12 M, pH 7.4), washed extensively in cacodylate buffer and then post-fixed for 1 hour in 2 % OsO_4 in cacodylate buffer. Samples were then washed with buffer and dehydrated in ethanol, then infiltrated in propylene oxide for 15 minutes and subsequently overnight in a mixture of propylene oxide and Epon (1:1). After this infiltration the pellet of mitochondria were embedded in Epon and following polymerization (+ 60 °C for 24 hours) thin sections (80 nm) were prepared using an ultramicrotome (Leica Ultracut; Leica Microsystems GmBH, Wien, Austria). These sections were stained with saturated uranyl acetate for 5 minutes, washed and then stained with 3 mM lead citrate for 5 minutes. Finally, the sections were photographed using a transmission electron microscope TEM LEO 912 (Advanced Light and Electron Microscopy BioImaging Center - San Raffaele Scientific Institute).

3.2.9 Statistical analysis

Statistical significance was determined by Student's t-test, considering the data with $p < 0.05$ as significant. The histograms represent the mean values obtained, and the bars indicate the standard deviation or standard error of the mean. Enzyme assays data were expressed as mean ± SEM. All the means were obtained from eight independent experiments with two replicas per assay. Considering that human brain samples were used for this study, a limited amount of samples was available and then has prevented us to perform a larger number of replicas. GRP75 western blot was expressed as mean ± SD and obtained from 3 independent experiments. All the values obtained from mitochondrial fractions were averaged and normalized on the averaged values obtained from brain homogenates.

4. Results

4.1 Morphological of mitochondria isolated from post mortem human brain cortex by using Sims and Anderson protocol

In order to evaluate the yield of Sims and Anderson method [180], mitochondria have been isolated following the same steps starting from post mortem brain tissue. The mitochondrial fraction was evaluated through transmission electron microscopy to get a rough view of their morphology and to estimate the possible contaminations. In figure 11 it is evident that the isolated human post mortem brain mitochondria are predominantly enclosed into synaptosomes together with many other cell components. Considering this result, which is far from the desired purity of mitochondria required for our purpose, the main effort of the study was to develop a new method to obtain a highly purified mitochondrial fraction from human post mortem tissues.

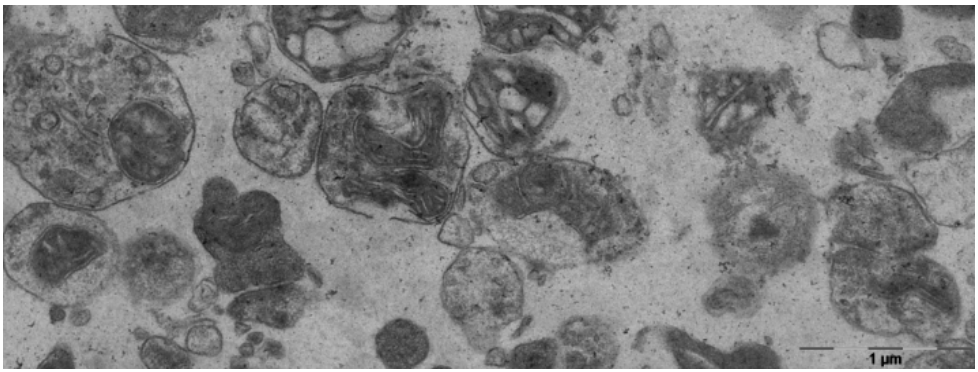

Figure 11: Representative electron micrograph showing a mitochondrial pellet to display the characteristic morphology

4.2 Analysis of mitochondria isolated from post mortem human brain cortex with the new developed method

The purity and integrity of the isolated mitochondria were analyzed using different techniques, as described below. The total protein content of the mitochondrial fraction was 377.06 µg ± 117.96 /g of tissue wet weight (mean ± SD; n= 8), as determined by Lowry's assay.

4.2.1 Enzymatic assay of mitochondrial fractions

Firstly, several enzymatic markers were selected for the investigation of mitochondrial enrichment and the presence of the major contaminants (Fig.12). When normalized to total protein concentrations, CS activity exhibited an increase of 4.75 ± 0.33-fold purification (mean ± SEM; n= 8), compared with the value of brain homogenates. Regarding contaminants, it can be observed that LDH activity, used as a synaptosomal marker, was very low in the final pellets (0.03 ± 0.005-fold) compared to LDH activity in brain homogenates. Instead, AP activity, used as assay for lysosomal contamination, showed a similar value in the enriched mitochondria fractions compared to brain homogenates (1.05 ± 0.07-fold). Peroxisomal contamination appears to be at low levels since CAT activity was sensibly diminished in the final mitochondria pellet: indeed CAT showed a purification fold of 0.58 ± 0.18 with respect to whole brain tissue homogenates. The evaluation of mitochondrial inner membrane intactness in the final fractions was performed by calculating the ratio between the CS activity in absence of a detergent buffer (Triton X-100^{TM}) versus the activity in the same mitochondria preparation in presence of a detergent buffer. Indeed, the CS enzyme is localized in

the mitochondrial matrix and its specific activity would not be correctly measured if the CS were not released by the rupture of mitochondrial membranes in presence of the detergent. This ratio was estimated to be 29.01 ± 3.65 % (mean ± SEM), thus demonstrating that the majority of mitochondria remained intact at the end of the protocol.

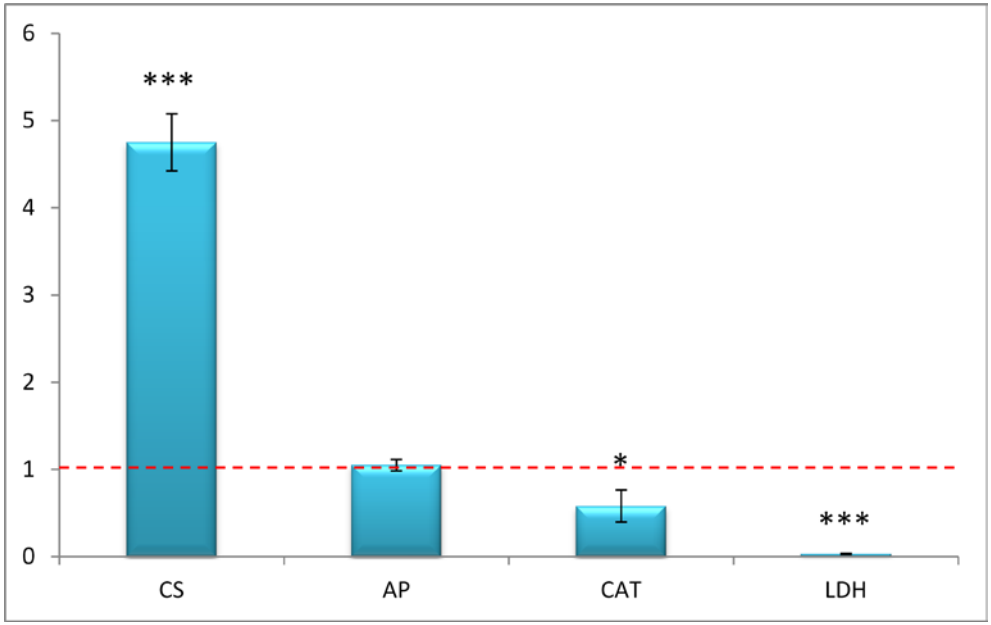

Figure 12. The histogram shows the mean purification fold values (mean ± SEM) of four different markers, normalized over brain homogenates (BH) (red dashed line). * = p value < 0.05 vs BH; *** = p value < 0.001 vs BH

4.2.2 Western blot of mitochondrial fractions

It was decided to proceed with further analysis using western blots, if no enzymatic assays were available. Western blots of isolated mitochondria (Fig. 13) demonstrated the absence of nuclear contamination (evaluated by H3 levels), while showed presence of the endoplasmic reticulum marker (PDI), which seems to be enriched in mitochondrial fractions, suggesting the presence of mitochondria-associated membranes (MAM). To confirm this hypothesis, some of the samples in which PDI was detected, were subjected to a specific analysis of a MAM marker (GRP75) by mean of western blot (Fig 14). These experiments showed a statistically significant increase of GRP75 (1.57 ± 0.32; mean ± SD; n = 4; p value < 0.05 vs BH), thus confirming of a MAM enrichment. Additionally, to verify if plasma membrane was absent in our mitochondrial fraction, western blot of two focal adhesion proteins were measured (Paxillin and PYK2). Figure 13 shows little or no plasma membrane contamination in purified mitochondria (Fig.15).

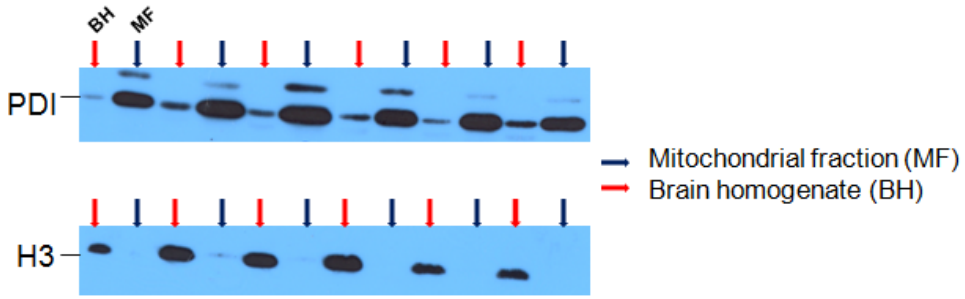

Figure 13. Western blot analyses of PDI and histone H3 on BH and MF obtained from six independent experiments.

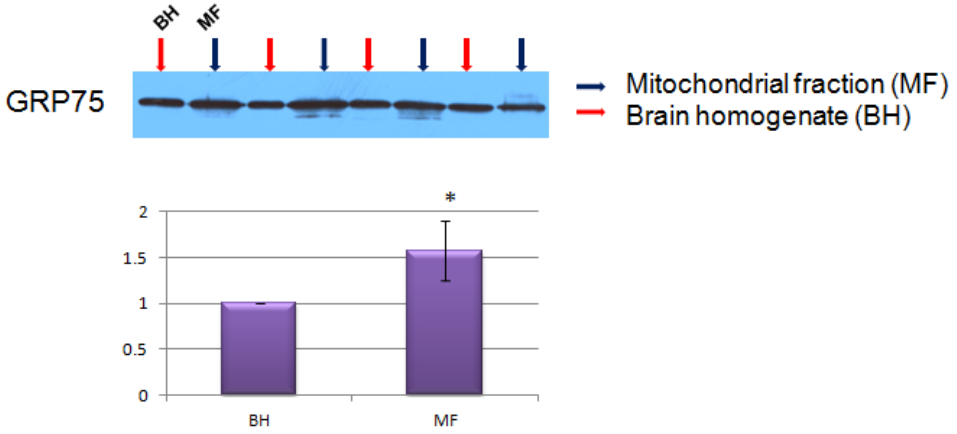

Figure 14. Western blot analyses of protein GRP75 on BH MF obtained from four independent experiments (mean ± SD; n = 4). The histogram shows densitometry analysis of mean values. * = p value < 0.05 vs BH

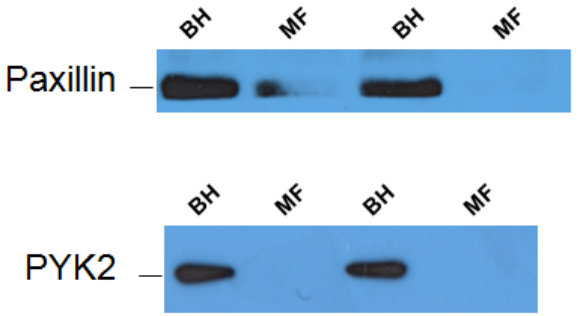

Figure 15. Western blot analyses of proteins Paxillin and PYK2 on BH and MF, obtained from two independent experiments.

4.2.3 Transmission electron microscopy of mitochondrial fractions

Evaluation of ultrastructure of the isolated mitochondria is presented in Fig. 16 (*panels* A, B). The presence of intact mitochondrial membranes demonstrated that the mitochondrial isolation procedure did not rupture or displace the membranes. Moreover, as it can be noticed from *panel* C (Fig.16), mitochondrial membranes bind to MAM micro domains, a further evidence of their presence in isolated mitochondria as demonstrated by western blots of typical MAM markers.

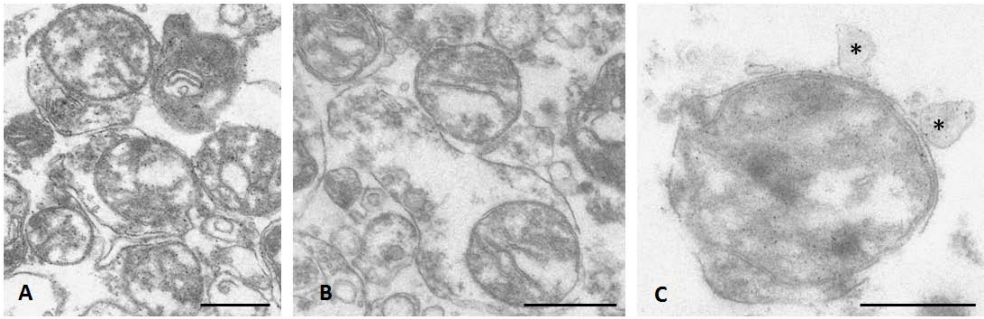

Figure 16. Representative electron micrographs showing the morphology of isolated mitochondria. These mitochondria were isolated from premotor cortex of a healthy subject (51 y.o.). Asterisks mark MAM vesicles juxtaposed to mitochondrial membranes. (Scale bar = 0.5μm).

4.3. Application of the new developed method for mitochondrial lipid analyses

4.3.1 Analysis of mitochondrial total lipid extract

After total lipid extraction, a relatively small quantity of sample has been analyzed after chromatographic run. This pilot experiment allowed us to observe different bands positive for anisaldehyde, a reagent for the non-selective detection of lipids (Fig.17). In MF, two major bands correspond to PE and PC, while the darker band at the beginning of the chromatographic run may be attributed to sucrose and mannitol present in MIB.

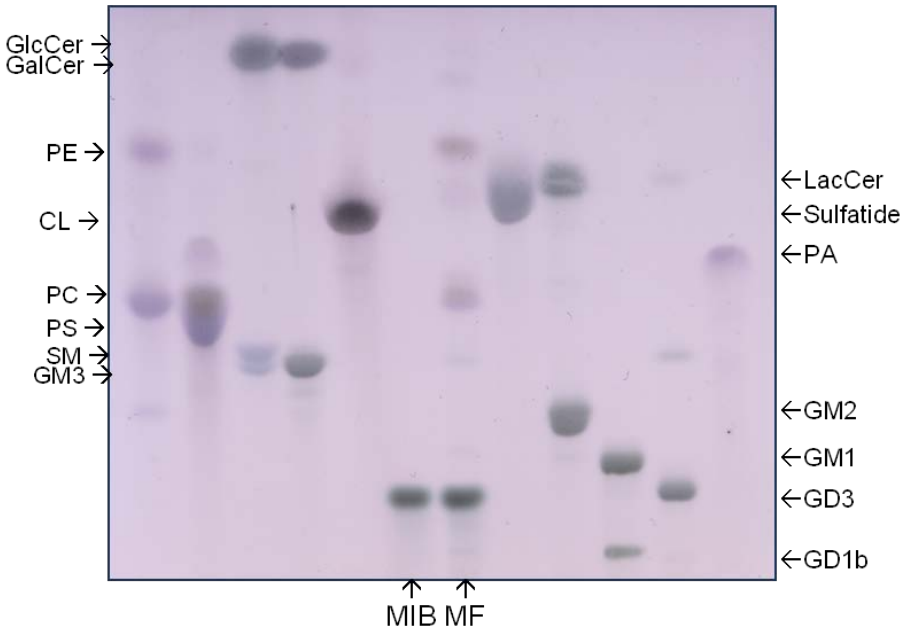

Figure 17. TLC analysis before microdialysis of total lipid extracts from isolated mitochondria (mitochondria isolated from a healthy subject of 50 y.o.). MF and MIB were subjected to lipid extraction with $CHCl_3/CH_3OH/H_2O$ 20:10:1 (v/v/v) and loaded (40 µg of protein) on a silica gel TLC plate. HPTLC was performed using chloroform/methanol/0.2% calcium chloride 60:35:8 (v/v/v) as solvent system. The lipids were then revealed using anisaldehyde as colorimetric detection.

4.3.2 Analysis of mitochondrial organic phase

A single mitochondria isolation did not produce sufficient amount of sample to perform the following analyses, so it was decided to pool multiple preparations and process the samples as one. After two-phase partitioning of total lipid extracts, samples were subjected to microdialysis to remove contaminating salts and sugars. The organic phase was resolved in different lipid classes and stained with two reagents, one for general detection of lipids (Fig. 18) and one specific for phospholipids (Fig. 19). In the first plate (Fig. 18) MF displays different bands corresponding to GalCer, PE, CL, PC, PI, PS and SM. To confirm the presence of phospholipids in MF, the second plate was stained for phosphorus detection (Fig.18): in this plate, blue specific bands appear corresponding to PE, CL, PC, PI, PS and SM. Beside demonstrating a considerable bandwidth for PE and PC, indicating a high number of phospholipids species, it should be emphasized the presence of CL, the signature phospholipid of mitochondria.

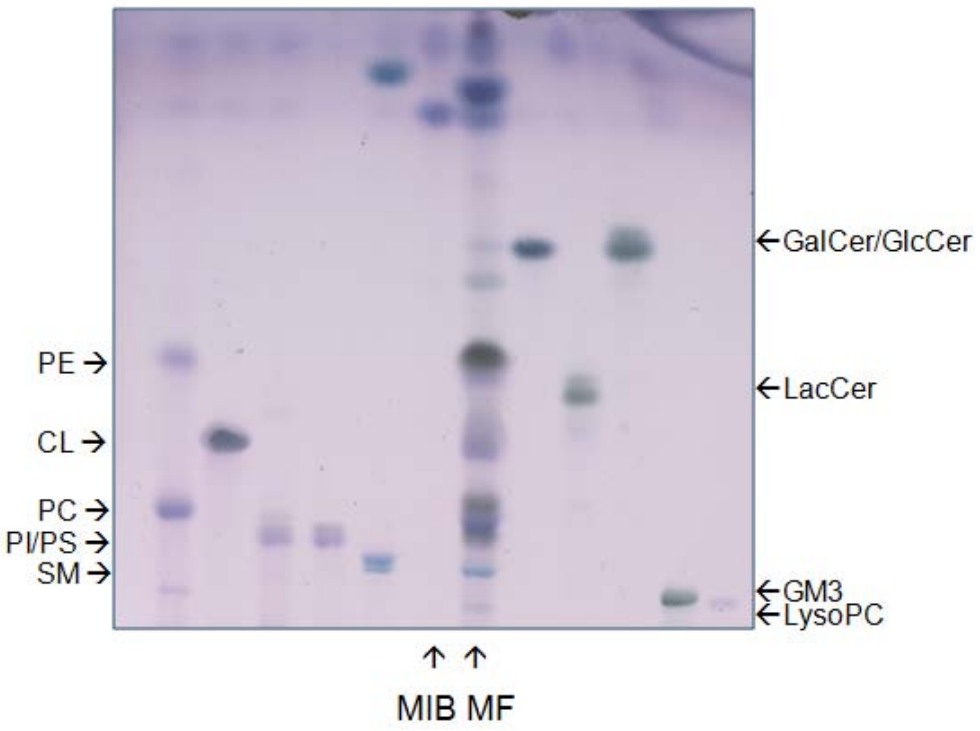

Figure 18. TLC analysis after microdialysis of organic phases from isolated mitochondria (9 pooled preparations, mitochondria isolated from healthy subjects with an age range 30-77 y.o.). Mitochondrial fraction (MF) and mitochondria isolation buffer (MIB) were subjected to lipid extraction with $CHCl_3/CH_3OH/H_2O$ 20:10:1 (v/v/v) and loaded (150 µg of protein) on a silica gel TLC plate. HPTLC was performed using $CHCl_3/CH_3OH/H_2O$ 110:40:6 (v/v/v) as solvent system. The lipids were then revealed using anisaldehyde as colorimetric detection.

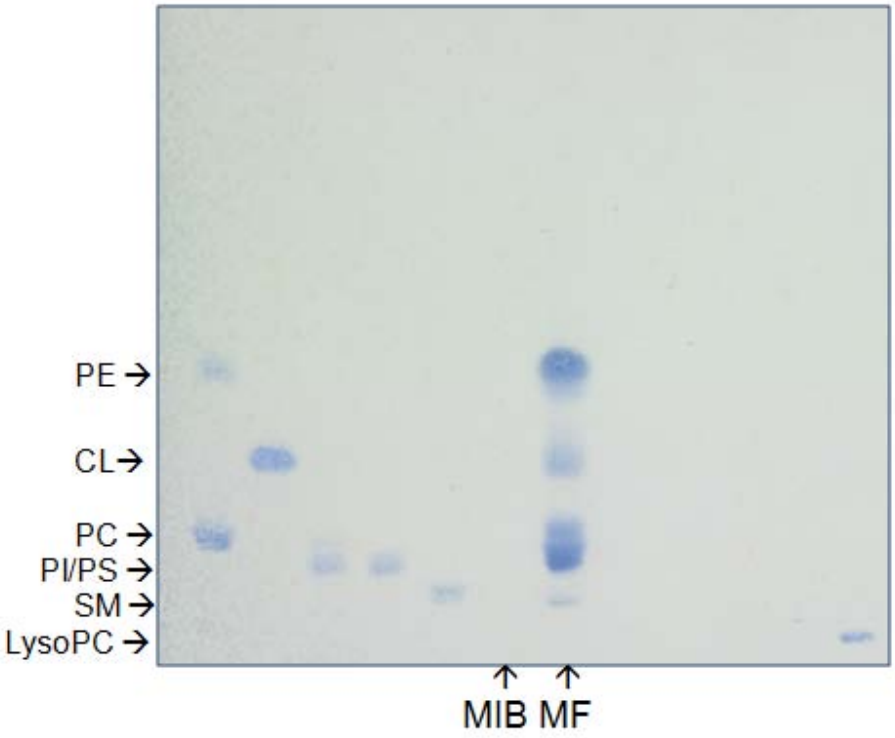

Figure 19. TLC analysis after microdialysis of organic phases from isolated mitochondria (9 pooled preparations, mitochondria isolated from healthy subjects with an age range 30-77 y.o.). MF and MIB were subjected to lipid extraction with $CHCl_3/CH_3OH/H_2O$ 20:10:1 (v/v/v) and loaded (150 µg of protein) on a silica gel TLC plate. HPTLC was performed using $CHCl_3/CH_3OH/H_2O$ 110:40:6 (v/v/v) as solvent system. The lipids were then revealed using a spray specific for phosphorus containing lipids as colorimetric detection.

4.3.2.1 2D-TLC

To obtain a better resolution of phospholipids classes, two-dimensional HPTLC was performed in two plates (Fig. 20). This approach allowed us to separate all spots, and make the CL more visible with respect to mono-dimensional TLC.

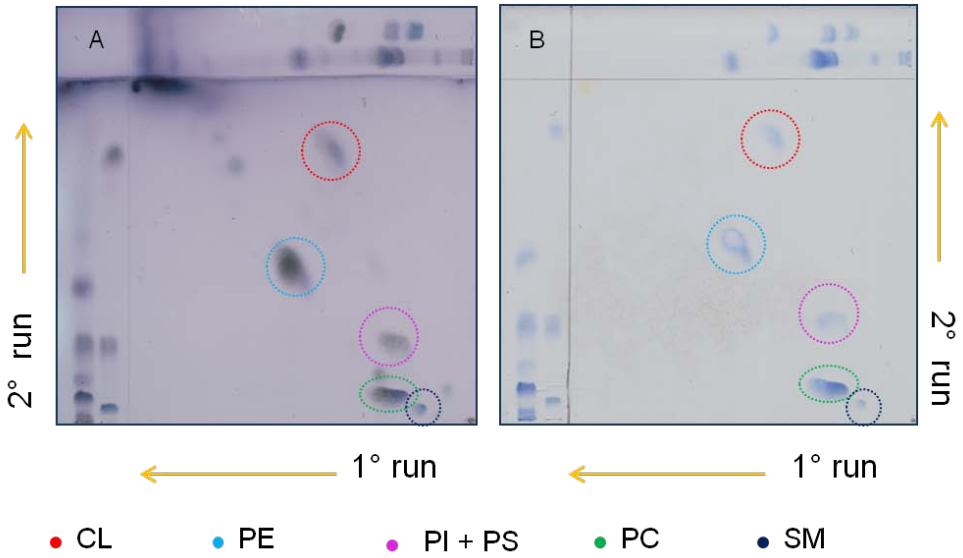

Figure 20. 2D-TLC analyses after microdialysis of organic phases from isolated mitochondria (9 pooled preparations, mitochondria isolated from healthy subjects with an age range 30-77 y.o.). MF were subjected to lipid extraction with $CHCl_3/CH_3OH/H_2O$ 20:10:1 (v/v/v) and loaded (200 µg of protein) on two a silica gel TLC plates. Two-dimensional HPTLC were performed using two different solvent systems: $CHCl_3/CH_3OH/H_2O$ 14:6:1 (v/v/v) for the first separation and $CHCl_3/CH_3OH/CH_3COOH$ 13:5:2 (v/v/v) for the second separation. The lipids were then revealed using anisaldehyde (*panel* A) and a spray specific for phosphorus containing lipids (*panel* B) as colorimetric detection.

4.3.2.2 Cholesterol quantitation

A simple method for cholesterol quantitative determination in MF was developed. The solvent system was specific for resolving exclusively cholesterol and a set of standard samples of known concentration was used to plot a calibration curve (Fig. 21). Thus, MF was loaded in double (15µg and 25µg) and bands were quantified through densitometric analysis. Cholesterol content was estimated to be 64.20 ± 1.99 nmol/mg of protein (mean ± SD).

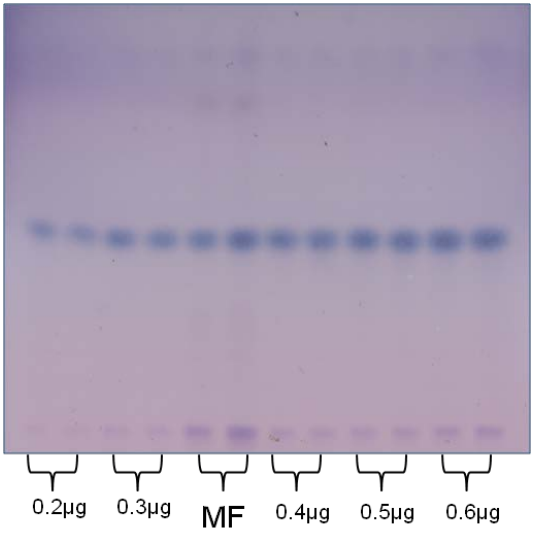

Figure 21. TLC analyses after microdialysis of organic phases from isolated mitochondria (9 pooled preparations, mitochondria isolated from healthy subjects with an age range 30-77 y.o.). MF were subjected to lipid extraction with $CHCl_3$:CH_3OH:H_2O 20:10:1 (v/v/v) and loaded (30 µg of protein) on a silica gel TLC plates, along with a set of cholesterol standard samples of known concentration. HPTLC was performed using C_6H_{14}/$C_4H_8O_2$ 3:2 (v/v), and cholesterol was then revealed using anisaldehyde as colorimetric detection.

4.3.3 Analysis of mitochondrial methanolyzed organic phases for glycolipids detection

Aliquots of the organic phases were then subjected to alkali treatment to selectively remove phospholipids and observe glycolipids. Also in this case we use two identical plates sprayed with two different reagents, one for general detection of lipids and one specific for glycolipids (Fig.22). In the case of aniline (Fig. 22B), a reagent that detects glycolipids by staining them in blue, the analysis revealed the presence of faint glycolipid patterns in MF. Then, in order to discriminate between GalCer and GlcCer in MF, we used a TLC plate pre-treated with $Na_2B_4O_7$ (4 %) and a specific solvent system. As it can be seen in Fig. 23, GalCer is present in MF.

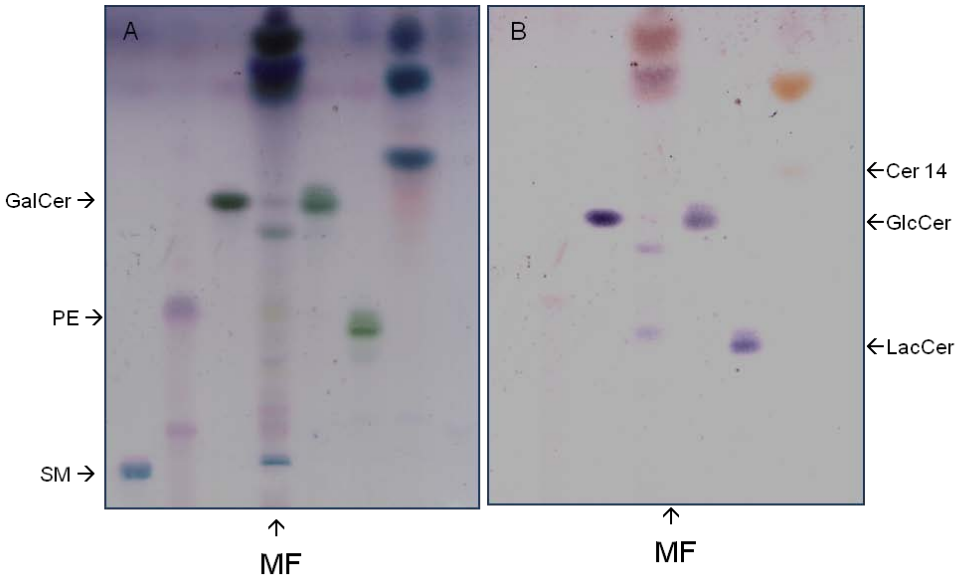

Figure 22. TLC analyses after microdialysis of methanolyzed organic phases from isolated mitochondria (9 pooled preparations, mitochondria isolated from healthy subjects with an age range 30-77 y.o.). MF were subjected to lipid extraction with $CHCl_3/CH_3OH/H_2O$ 20:10:1 (v/v/v) and loaded (250 µg of protein) on two a silica gel TLC plates. HPTLC was performed using $CHCl_3/CH_3OH/H_2O$ 110:40:6 (v/v/v) as a solvent system. The lipids were then revealed using anisaldehyde (*panel* A) and aniline (*panel* B) as colorimetric detection.

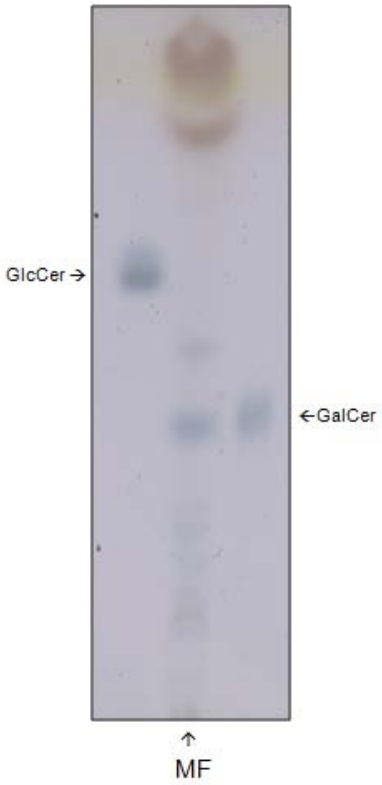

Figure 23. TLC analyses after microdialysis of methanolyzed organic phases from isolated mitochondria (9 pooled preparations, mitochondria isolated from healthy subjects with an age range 30-77 y.o.). MF were subjected to lipid extraction with $CHCl_3/CH_3OH/H_2O$ 20:10:1 (v/v/v) and loaded (260 µg of protein) on two a silica gel TLC plates. HPTLC was performed using $CHCl_3/CH_3OH/NH_3$ (2N) 70:30:3 (v/v/v) as a solvent system. The lipids were then revealed using and aniline as colorimetric detection.

4.3.3.1 Detection of ceramide

Using a specific solvent system, we evaluated the presence of ceramide molecules with different chain-lengths (C-12/-14/-16/-18/-22). As shown in Fig. 24, in MF there is no detectable ceramide with any of the aforementioned chain lengths.

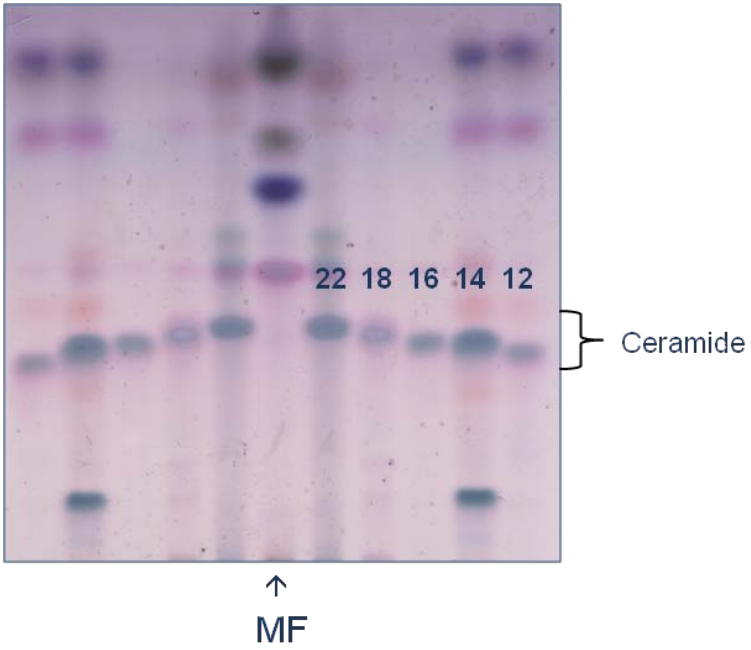

Figure 24. TLC analyses after microdialysis of methanolyzed organic phases from isolated mitochondria (9 pooled preparations, mitochondria isolated from healthy subjects with an age range 30-77 y.o.). MF were subjected to lipid extraction with $CHCl_3/CH_3OH/H_2O$ 20:10:1 (v/v/v) and loaded (120 µg of protein) on two a silica gel TLC plates. HPTLC for detection of ceramide was executed with $C_6H_{14}/CHCl_3/C_3H_6O/CH_3COOH$ 20:70:20:4 (v/v/v/v). The lipids were then revealed using anisaldehyde as colorimetric detection.

4.3.4 Analysis of mitochondrial aqueous phases to identify gangliosides

Following two-phase partitioning, aqueous phases were also spotted on a silica-gel TLC plate to obtain a proper separation of gangliosides. In a first attempt, before microdyalisis, we could not observe any glycosphingolipid. Indeed, Ehrlich's reagent, that is used to reveal sialic acid, stained only a sucrose/mannitol non specific band (Fig. 25) both in MF and MIB. After microdyalisis, the non specific band disappeared from MIB lane and ganglioside patterns were specifically colored by Ehrlich's reagent (Fig. 26), thus demonstrating that microdialysis successfully removed sucrose and mannitol.

4.3.4.1 Immunostaining with Cholera β-toxin to confirm ganglioside presence

To validate that the previous observed bands were actually gangliosides, we decided to perform further experiment, using an immunostaining with cholera β-toxin after sample resolution. This approach, that allows a selective detection of gangliosides, corroborates preceding observation of a particular ganglioside pattern (Fig. 27), that characterize MF aqueous phases.

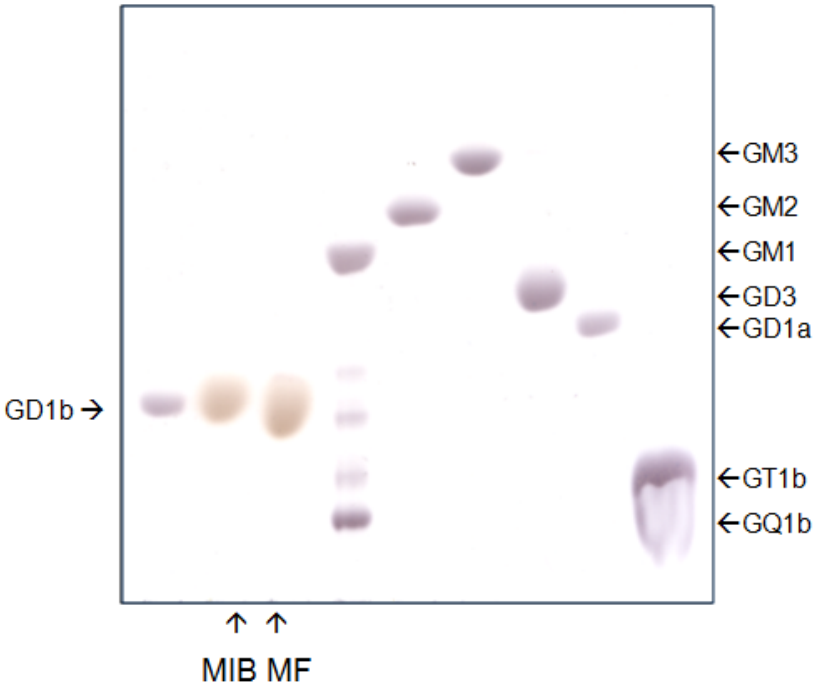

Figure 25. TLC analysis before microdialysis of aqueous phases from isolated mitochondria (9 pooled preparations, mitochondria isolated from healthy subjects with an age range 30-77 y.o.). MF and MIB were subjected to lipid extraction with $CHCl_3/CH_3OH/H_2O$ 20:10:1 (v/v/v) and loaded (150 µg of protein) on a silica gel TLC plate. HPTLC was performed using $CHCl_3/CH_3OH/CaCl_2$ (0.2 %) 50:42:11 (v/v/v) as solvent system. The lipids were then revealed using Ehrlich's reagent as colorimetric detection.

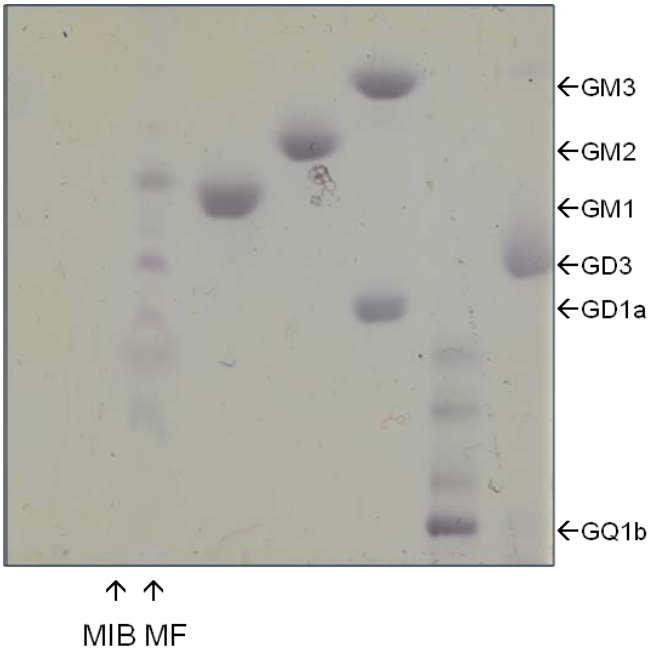

Figure 26. TLC analysis after microdialysis of aqueous phases from isolated mitochondria (9 pooled preparations, mitochondria isolated from healthy subjects with an age range 30-77 y.o.). MF and MIB were subjected to lipid extraction with $CHCl_3/CH_3OH/H_2O$ 20:10:1 (v/v/v) and loaded (150 µg of protein) on a silica gel TLC plate. HPTLC was performed using using $CHCl_3/CH_3OH/CaCl_2$ (0.2 %) 50:42:11 (v/v/v) as solvent system. The lipids were then revealed using Ehrlich's reagent as colorimetric detection.

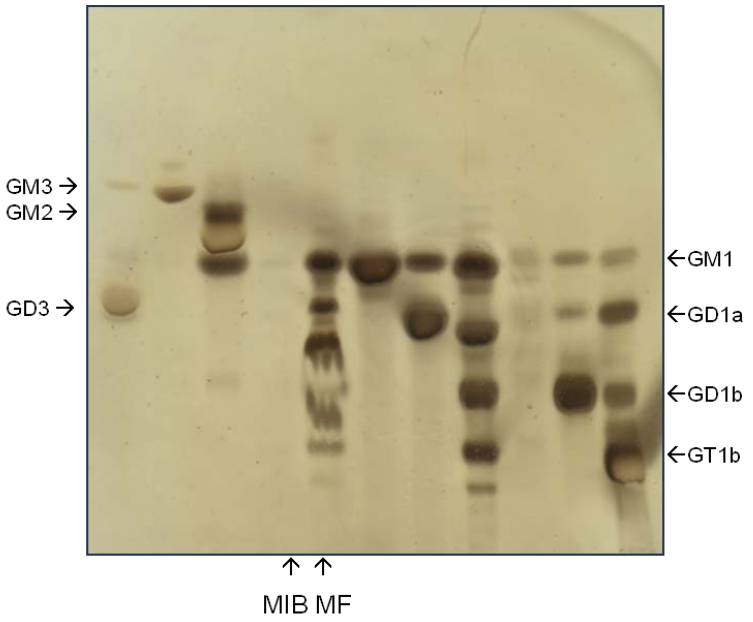

Figure 27. TLC analysis after microdialysis of aqueous phases from isolated mitochondria (9 pooled preparations, mitochondria isolated from healthy subjects with an age range 30-77 y.o.). Mitochondrial fraction (MF) and mitochondria isolation buffer (MIB) were subjected to lipid extraction with $CHCl_3/CH_3OH/H_2O$ 20:10:1 (v/v/v) and loaded (200 µg of protein) on a silica gel TLC plate. HPTLC was performed using using $CHCl_3/CH_3OH/CaCl_2$ (0.2 %) 50:42:11 (v/v/v) as solvent system. Gangliosides were detected by TLC-immunostaining with cholera toxin after treatment with sialidase.

4.4. Mitochondrial lipid analyses in physiological brain aging

4.4.1 Analysis of mitochondrial organic phases in aging

After developing a plan to study main lipid classes characterizing previously isolated mitochondria, we decided to compare mitochondrial lipid compositions of a young subject and of an old subject. We started with organic phases comparison (Fig. 28) and noticed a visible decrease of SM, neutral glycolipids and cholesterol in the older subject's MF, while PE and PC remained basically constant. We also analyzed phospholipid species (Fig. 29) and, interestingly, we found a different pattern between the two subjects. Moreover, we were able to measure cholesterol content quantifying bands through densitometric analysis (Fig. 30) obtaining a value of 58.81nmol/mg protein in the young subject's MF and a value of 32.57nmol/mg protein. This data reveals a substantial loss of cholesterol content in mitochondria through human brain aging.

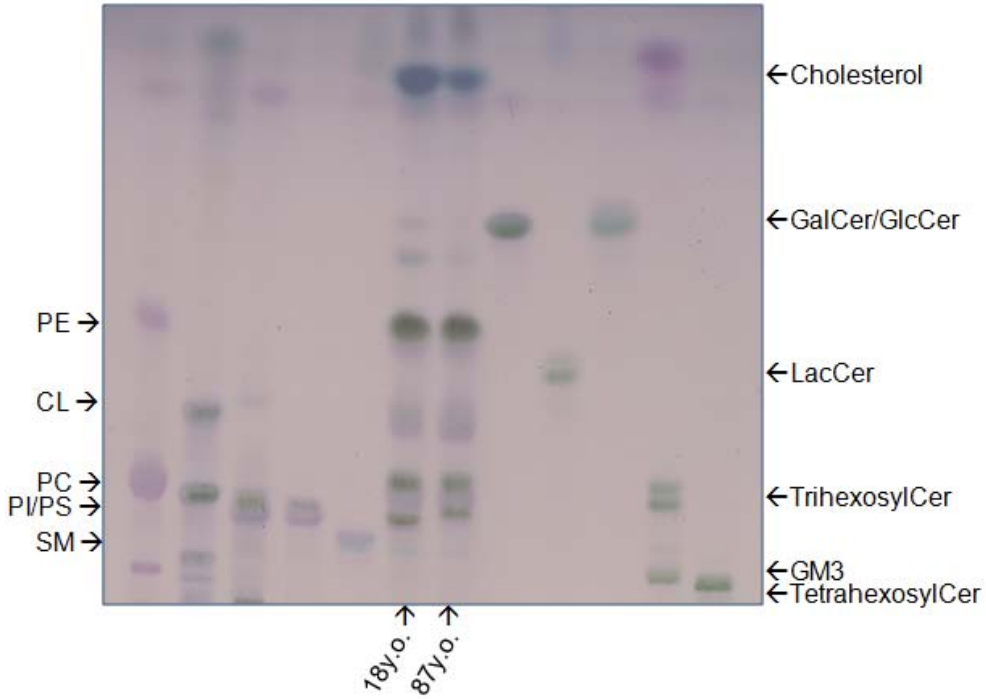

Figure 28. TLC analysis after microdialysis of organic phases from mitochondria isolated from two different subjects. The MF isolated from two subjects of 18 y.o. and 87 y.o. were subjected to lipid extraction with $CHCl_3/CH_3OH/H_2O$ 20:10:1 (v/v/v) and loaded (100 µg of protein) on a silica gel TLC plate. HPTLC was performed using $CHCl_3/CH_3OH/H_2O$ 110:40:6 (v/v/v) as solvent system. The lipids were then revealed using anisaldehyde as colorimetric detection.

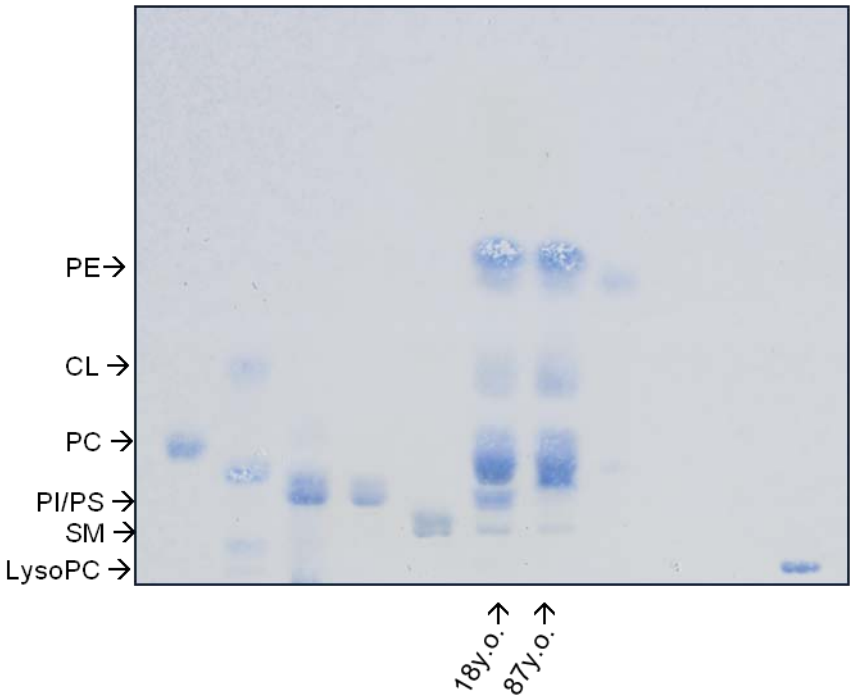

Figure 29. TLC analysis after microdialysis of organic phases from mitochondria isolated from two different subjects. The MF isolated from two subjects of 18 y.o. and 87 y.o. were subjected to lipid extraction with $CHCl_3/CH_3OH/H_2O$ 20:10:1 (v/v/v) and loaded (150 µg of protein) on a silica gel TLC plate. HPTLC was performed using $CHCl_3/CH_3OH/H_2O$ 110:40:6 (v/v/v) as solvent system. The lipids were then revealed using a spray specific for phosphorus containing lipids as colorimetric detection.

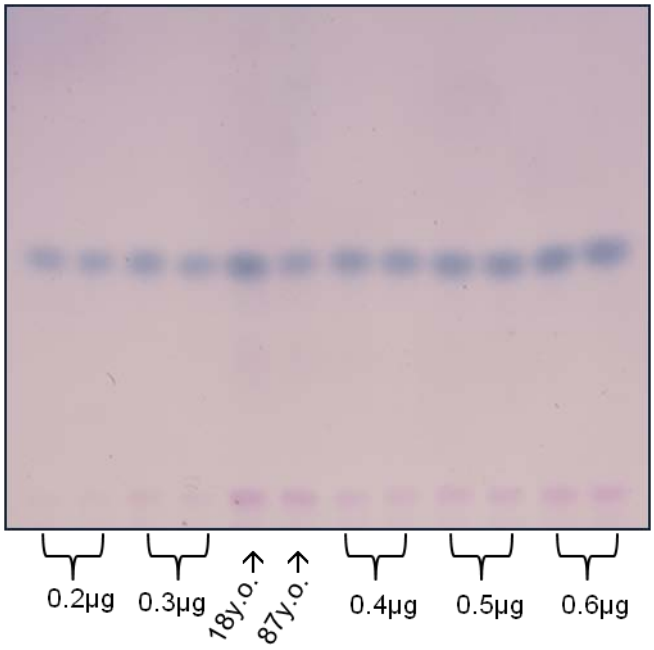

Figure 30. TLC analysis after microdialysis of organic phases from mitochondria isolated from two different subjects. The MF isolated from two subjects of 18 y.o. and 87 y.o. were subjected to lipid extraction with $CHCl_3$:CH_3OH:H_2O 20:10:1 (v/v/v) and loaded (30 µg of protein) on a silica gel TLC plates, along with a set of cholesterol standard samples of known concentration. HPTLC was performed using C_6H_{14}/$C_4H_8O_2$ 3:2 (v/v), and cholesterol was then revealed using anisaldehyde as colorimetric detection.

4.4.2 Analysis of mitochondrial methanolyzed organic phases for glycolipids detection in aging

A comparison between the two methanolyzed organic phases was performed by running two identical plates sprayed with two different reagents (as previously explained). Figure 31 highlights a visible decrease in glycolipid classes in the old subject's MF both with anisaldehyde (*panel* A) and aniline (*panel* B) (Fig.31) reagents.

4.4.3 Analysis of mitochondrial aqueous phases for gangliosides detection in aging

Aliquots of the aqueous phases were then spotted on two silica-gel TLC plates in order to evaluate possible age-related changes in gangliosides components of MF. In Figure 32 there is a remarkable difference between MF of different ages, since in the older subject no bands were colored (Fig. 32). Furthermore, with TLC immunostaining, which is a far more sensitive technique, a similar ganglioside pattern can be observed, but a lower content in all gangliosides species (GM1, GD1a, GD1b, GT1b, GQ1b) present in the older subject's MF than in the young subject's MF (Fig. 33).

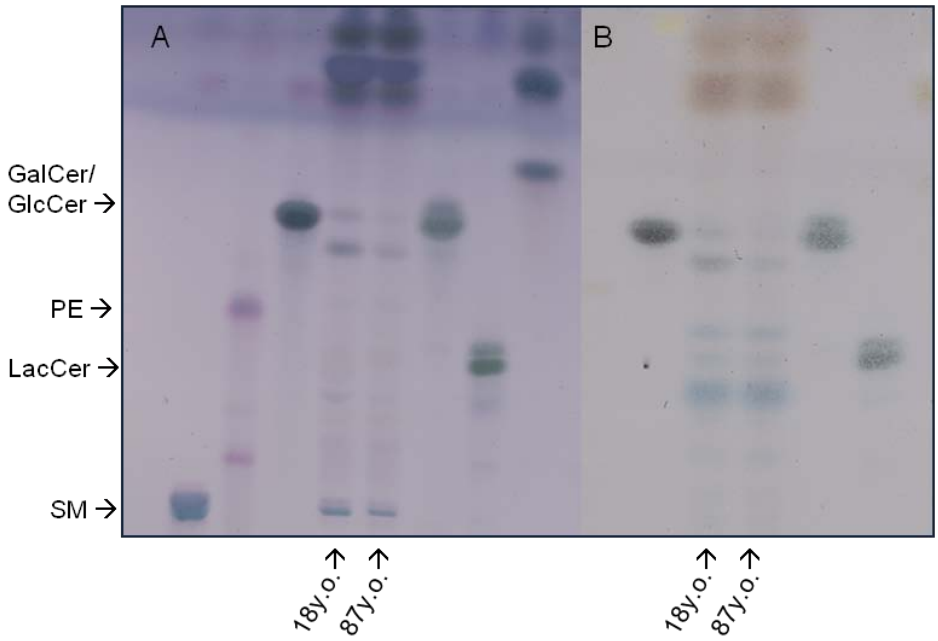

Figure 31. TLC analysis after microdialysis of methanolyzed organic phases from mitochondria isolated from two different subjects. The MF isolated from two subjects of 18 y.o. and 87 y.o. were subjected to lipid extraction with $CHCl_3/CH_3OH/H_2O$ 20:10:1 (v/v/v) and loaded (150 µg of protein in *panel* A and 200µg in *panel* B) on two a silica gel TLC plates. HPTLC was performed using $CHCl_3/CH_3OH/H_2O$ 110:40:6 (v/v/v) as a solvent system. The lipids were then revealed using anisaldehyde (*panel* A) and aniline (*panel* B) as colorimetric detection.

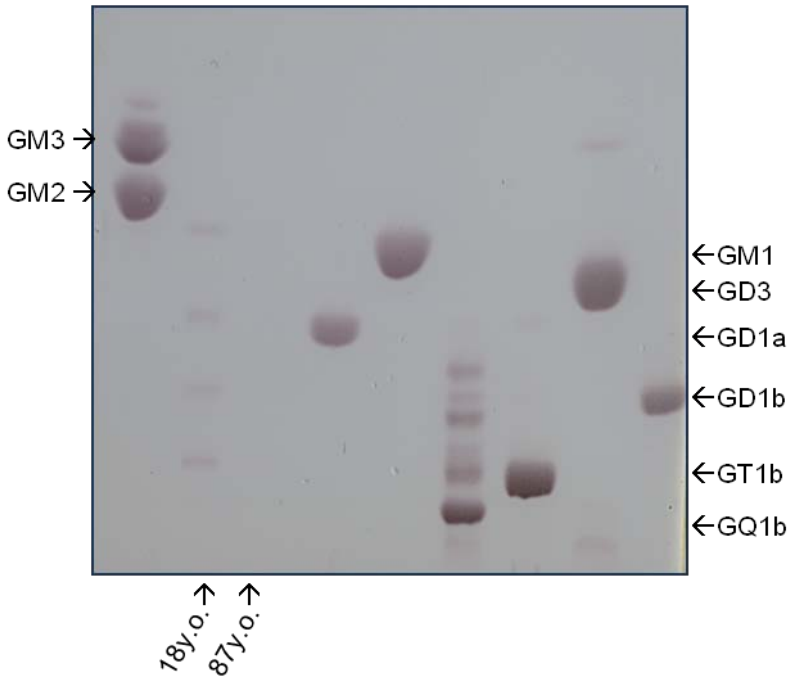

Figure 32. TLC analysis after microdialysis of aqueous phases from mitochondria isolated from two different subjects. The MF isolated from two subjects of 18 y.o. and 87 y.o. were subjected to lipid extraction with $CHCl_3/CH_3OH/H_2O$ 20:10:1 (v/v/v) and loaded (170 µg of protein) on a silica gel TLC plate. HPTLC was performed using $CHCl_3/CH_3OH/CaCl_2$ (0.2 %) 50:42:11 (v/v/v) as solvent system. The lipids were then revealed using Ehrlich's reagent as colorimetric detection.

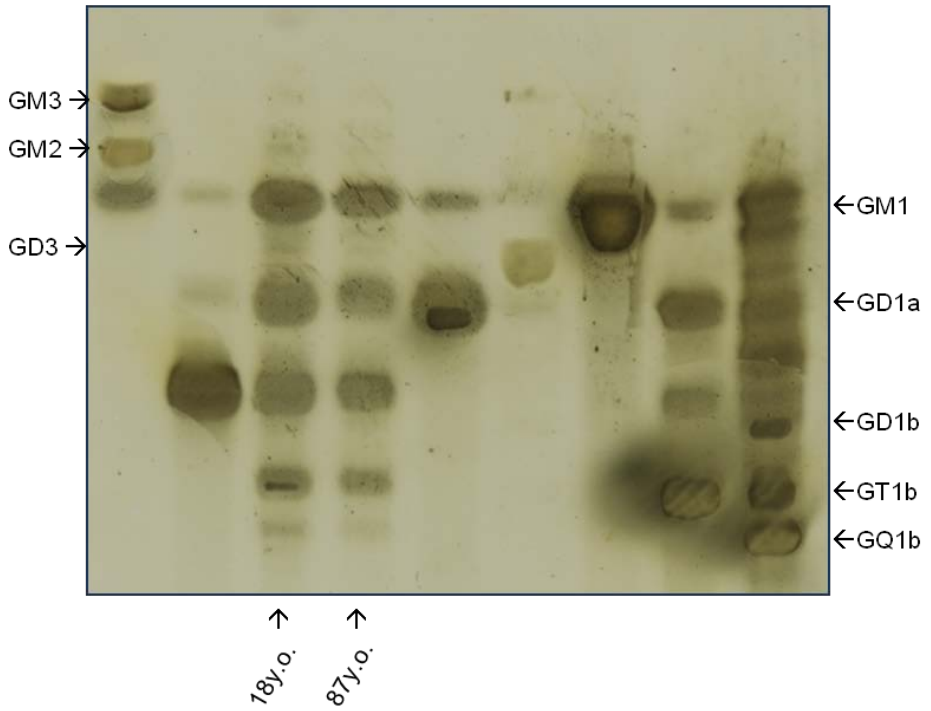

Figure 33. TLC analysis after microdialysis of aqueous phases from mitochondria isolated from two different subjects. The MF isolated from two subjects of 18 y.o. and 87 y.o. were subjected to lipid extraction with $CHCl_3/CH_3OH/H_2O$ 20:10:1 (v/v/v) and loaded (200 µg of protein) on a silica gel TLC plate. HPTLC was performed using $CHCl_3/CH_3OH/CaCl_2$ (0.2 %) 50:42:11 (v/v/v) as solvent system. Gangliosides were detected by TLC-immunostaining with cholera toxin after treatment with sialidase.

5. Discussion

Mitochondria are cytoplasmic lipid-rich organelles delimited by a double membrane, with the external side in contact with the cytoplasm and the internal side that folds over many times and creates layered structures called “cristae”. Mitochondria do not only represent the cellular power plant but they also play a key role in other crucial functions, such as the intrinsic pathway of apoptosis. The central nervous system requires high ATP consumption to perform its characteristic functions, thus the loss of the mitochondria dynamic balance may lead to neuronal damage. Their involvement in brain aging is widely acknowledged by numerous studies [62, 63]. Indeed, it has been observed that energy metabolism declines with age due to decreased activity of the mitochondrial respiratory chain complexes. In addition, the mitochondrial theory of aging postulated that mitochondria continue to produce reactive oxygen species within the cell and that this process leads to an increase in protein and lipid oxidation, and to an accumulation of mtDNA mutations [67]. Besides, there is an alteration of mitopagy [87], a selective process of macroautophagy that degrades dysfunctional or structurally damaged mitochondria. Finally, mitochondria are considered to be involved in cellular mechanisms that promote alterations both in physiological and pathological aging, such as chronic neurodegenerative diseases of the senile brain [63].

Mitochondria possesses two biochemically different membrane: the lipid components of the inner and outer mitochondrial membranes are not comparable. The outer mitochondrial membrane is fluid and contains higher levels of

cholesterol and PI. In contrast, the inner mitochondrial membrane is highly folded, enriched in PE and contains CL, a component synthesised and restricted to this membrane layer [193]. Furthermore, the actual relative ratio of various lipid components may vary with the age-related structural and functional changes of brain mitochondria [194]. For example, some factors as cholesterol/phospholipids molar ratio, phospholipids composition (i.e. CL), degree of fatty acid unsaturation, and lipid/protein ratio can affect the membrane fluidity and, consequently, protein activities and mitochondria functionality [195]. There is limited knowledge about the lipid composition of brain mitochondria compared to other tissues, such as the liver and the heart. In particular, the lipid composition of human brain mitochondria is poorly characterized.

To characterize the lipid species within human brain mitochondria and evaluate if there are changes in their lipid composition through aging, we firstly had to obtain a reproducible and adequate isolation protocol to obtain highly purified mitochondria. To the best of our knowledge, present protocols for isolation of human brain mitochondria have been developed mainly modifying Sims and Anderson isolation protocol of rat brain mitochondria [180]. The preliminary study of the project was the application of this method to isolate mitochondria from post mortem human brain cortex. Unfortunately, results did not fulfil requirements since electron micrographs showed mitochondria encapsulated inside synaptosomes (structures formed at the synaptic level during homogenization after opening and reclosing of the plasma membrane), which is index of contamination by other cell components. Thus, the first aim of this study was to develop a satisfying and standardized method to extract highly purified mitochondria from frozen human brain cortex. For this purpose, validating biochemical assays such as enzymatic

assays had to be defined to assess mitochondria purity and integrity. To measure mitochondrial enrichment and integrity, CS was chosen as marker due to its localization inside the mitochondrial matrix. Reliable enzymatic assays of possible contaminants were then established according to comparable size and density of mitochondria. The evaluation of the contamination by synaptosomes, lysosomes and peroxisomes was assayed measuring respectively LDH activity, AP activity and CAT activity. Once the new protocol was developed, results from CS assays showed a 4.75-fold purification. As specific subcellular populations are purified, unique markers of these structures should be enriched. The enrichment from the total homogenate depends on the proportion of the homogenate occupied by the particles. For example, if 20 % of the homogenate is represented by mitochondria, as in the case of liver [195], a maximum enrichment of 5-fold is expected. Precise data are not available in the relative composition of brain homogenates, but it has been reported that isolated mitochondria from rat neurons (primary culture) showed a citrate synthase activity increased by 4-fold [197]. Considering these data, it can be pointed out that we obtained a satisfying enrichment.

If we consider contaminations we found, AP showed an activity of 1.05-fold while CAT activity was 0.58-fold with respect to whole brain tissue homogenate. Lisman and colleagues reported a purification of rat brain lysosomes with 7-10-fold over the homogenate [198] while Kovacs and co-workers achieved a peroxisomal fraction purification at least 40-fold over the original mouse brain homogenate [199]. Comparing these values, it can be observed that peroxisomal contamination was definitely low, and lysosomes presence may be estimated to about 10 % of our mitochondrial fraction. Moreover, since LDH value was close to zero (0.03-fold), a significative synaptosomal contamination can be excluded.

When any enzymatic assay was unavailable, contamination from other cell components was evaluated by using western blots. Results demonstrated there was not nuclear or plasma membrane contamination, but there was an endoplasmic reticulum marker which seemed to be enriched in mitochondrial fractions. Therefore, we hypothesized that MAM could have been conserved throughout the isolation procedure. MAM are dynamic platforms in close apposition between mitochondria and endoplasmic reticulum (Fig. 34), that are implicated in fundamental cellular processes, such as lipid biosynthesis and transport, Ca^{2+} signalling, energy metabolism, cell survival and apoptosis [31]. Electron microscopy results actually showed not only mitochondrial membranes integrity, but also the presence of MAM vesicles juxtaposed to mitochondrial membranes. To verify our hypothesis, we performed a western blot quantifying GRP75, a MAM marker protein that strengthens the functional interaction between the ER and mitochondria by forming a ternary bridging complex [200]. Experiments showed a statistically significant increase of GRP75 in mitochondrial fractions and a confirmation of MAM enrichment.

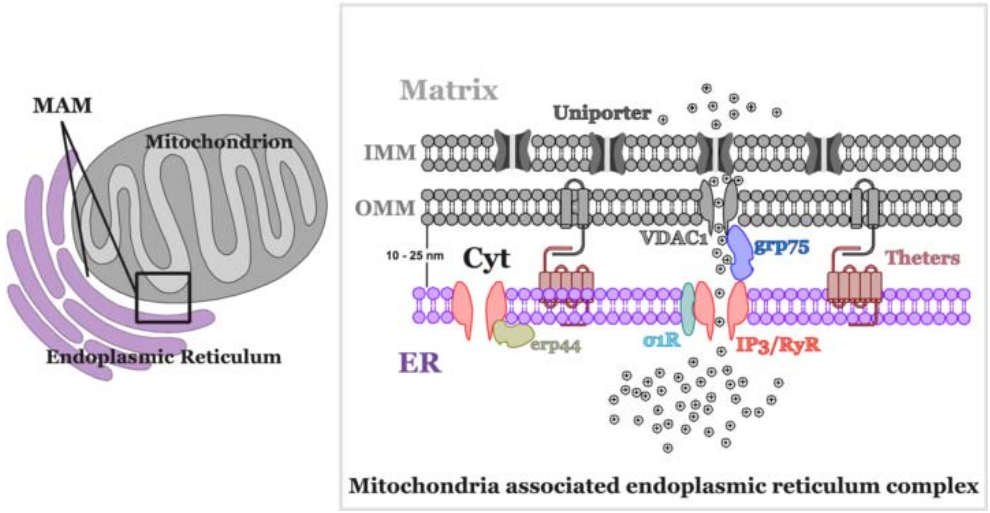

Figure 34. Schematic representation of mammalian MAM with some of the proteins localized at the contact site. GRP75 (blue) bridges the gap between IP3R and VDAC [200]. (Source: https://frombenchtobedside.wordpress.com/2014/03/03/introduction-to-mitochondria-part-1/)

To investigate the lipid composition of highly purified mitochondria, lipid extracts were partitioned into organic and aqueous phases. The analysis of organic phases performed by HPTLC revealed the prevalence of phospholipids species (PE, PC, SM, CL, PI, PS), as previously demonstrated in mitochondria deriving from different tissue types [201]. We detected also cholesterol and glycosphingolipids such as GalCer and gangliosides, that are generally assumed to be localized primarily (approx. 80%) in the plasma membrane [202]. Since we did not find reliable information about lipid composition of human brain mitochondria, we compared our data to those obtained from mouse brain mitochondria (Tab. 3) and noticed that the ratio between various molecules was very similar. Nevertheless, in

this study [169] gangliosides were found only in trace and other glycosphingolipids were not detected. Instead, Gillard and co-workers reported a variable subcellular localization of glycosphingolipids: interestingly, both anti-GalCer and monoclonal antibody A2B5, which binds polysialogangliosides, localized to mitochondria [203] in a wide variety of cell types. Moreover, TLC analyses of rat liver membranes revealed that gangliosides were present in mitochondria and endoplasmic reticulum as well [202]. Indeed, we can assume that the amount of gangliosides in our mitochondrial fractions could not be explained by contamination by plasma membrane, since our analyses showed no significant contamination. Furthermore, total homogenate ganglioside compositions is not similar [204], on a percent basis, to the pattern we detected in aqueous phases.

Finally, we conducted a pilot study of how mitochondria lipid composition may change in human aging, and noticed relevant differences as below explained. Indeed, we saw a visible decrease of SM and neutral glycolipids in the older subject compared to younger subject. PE and PC remained basically constant, but we observed a different phospholipid distribution pattern between the two subjects and a substantial loss of cholesterol content in mitochondria through human brain aging. It has to be underlined that mitochondrial phospholipids are critical throughout the autophagic process, from initiation and phagophore formation to elongation and fusion with endolysosomal vesicles [205], so it is convincing that the alteration of phospholipids species in brain aging could lead to neurodegeneration. Furthermore, it is known that cholesterol plays a key role in maintaining the membrane lipid bilayer architecture by regulating the mobility of phospholipids [206], and it is important to remark that the cholesterol content in human gray matter was reported to decrease in the oldest age group [207].

Consistently with our result, Ruggiero et al. [208] investigated the effect of aging on the lipid composition of rat brain mitochondria and found the same decrease in cholesterol content.

Moreover, our data showed that all gangliosides species (GM1, GD1a, GD1b, GT1b, GQ1b) displayed a lower bandwidth in the older subject. The study of Segler-Stahl et al. [209] demonstrated that ganglioside concentration decreases considerably in human brain, but this event could be explained by the loss of neurons and deterioration of synapses, which are known to occur in the physiological process of human aging [210].

The data obtained showed an evident relative biological difference. To confirm the results, it is clearly necessary to have a population statistic that needs an increasing of the subjects number.

6. Conclusions

Brain aging is a physiological process of structural and functional decay that occurs in different areas of the brain, depending on the lifestyle and predisposition of individuals. Major changes in the older brain include an important loss of neurons and dendritic trees in numerous regions of the cerebral cortex and hippocampus, a decrease in the volume of the gray substance, and an increase in ventricular volume. This process causes a cognitive decline that is more concerned with specific domains, such as visual and verbal memory. In the central nervous system, the cellular energy demand is surprisingly high, but as a person ages, his brain energy metabolism declines. Mitochondria are lipid-rich organelles involved in many and important cellular processes, but they are popularly known as the power house of the cell. These intriguing organelles are decisively involved in brain aging as well as in the onset or progression of several age-related neurodegenerative diseases. Thus, this project aimed to investigate the lipid composition of human brain mitochondria and to evaluate their changes in physiological aging, as no previous studies had been performed with this purpose. Firstly, in this study a new reliable and reproducible protocol has been developed to isolate highly pure mitochondria from post mortem human brain cortex; purity and integrity have been verified by biochemical assays and electron microscopy. Secondly, this protocol has been applied to study the lipid composition of mitochondrial fractions of human brain cortex, and finally, preliminary data have shown differences in mitochondria lipid composition during aging, suggesting a need of further investigation that will be employed by increasing the number of subjects. In conclusion, these data would offer a starting point for new studies, that eventually

will be used for the development of new pharmaceutical strategies targeted to decelerate aging process and prevent neurodegenerative diseases.

7. References

1. Kölliker, A. Z.Wiss. Zool. 1856. 8:311-325.
2. Altmann, R. Die Elementarorganismen und ihre Beziehungen zu den Zellen. Veit, Leipzig. 1890.
3. Sagan L. On the origin of mitosing cells. J Theor Biol. 1967 Mar;14(3):255-74.
4. Benda, C. "Ueber die Spermatogenese der Vertebraten und höherer Evertebraten, II. Theil: Die Histiogenese der Spermien".1898.
5. Pallen MJ. Time to recognise that mitochondria are bacteria? Trends Microbiol. 2011 Feb;19(2):58-64.
6. Mannella CA. Structure and dynamics of the mitochondrial inner membrane cristae. Biochim Biophys Acta. 2006 May-Jun;1763(5-6):542-8.
7. Yaffe MP. The machinery of mitochondrial inheritance and behavior. Science.1999 Mar 5;283(5407):1493-7.
8. Scheffler IE . Mitochondria (1st Edition), Wiley, New York. 1999
9. Krauss, S. Mitochondria: Structure and Role in Respiration. eLS. 2001
10. Passarella S, Atlante A, Valenti D, de Bari L. The role of mitochondrial transport in energy metabolism. Mitochondrion. 2003 Apr;2(5):319-43.
11. Lemasters JJ, Holmuhamedov E. Voltage-dependent anion channel (VDAC) as mitochondrial governator--thinking outside the box. Biochim Biophys Acta. 2006 Feb;1762(2):181-90.
12. Comte J, Maïsterrena B, Gautheron DC. Lipid composition and protein profiles of outer and inner membranes from pig heart mitochondria. Comparison with microsomes. Biochim Biophys Acta. 1976 Jan 21;419(2):271-84.
13. Hackenbrock, C. R. Ultrastructural bases for metabolically linked mechanical activity in mitochondria. I. Reversible ultrastructural changes with change in metabolic steady state in isolated liver mitochondria. J. Cell Biol. 1966. 30, 269–297
14. McCarron JG, Wilson C, Sandison ME, Olson ML, Girkin JM, Saunter C, Chalmers S. From structure to function: mitochondrial morphology, motion and shaping in vascular smooth muscle. J Vasc Res. 2013;50(5):357-71.
15. Perkins G, Renken C, Martone ME, Young SJ, Ellisman M, Frey T. Electron tomography of neuronal mitochondria: three-dimensional structure and organization of cristae and membrane contacts. J Struct Biol. 1997 Aug;119(3):260-72.

16. Daems, W. T., and Wisse, E. Shape and attachment of the cristae mitochondriales in mouse hepatic cell mitochondria. J. Ultrastruct. Res. 1966. 16, 123–140.
17. Taanman JW. The mitochondrial genome: structure, transcription, translation and replication. Biochim Biophys Acta. 1999 Feb 9;1410(2):103-23.
18. Gilchrist RB, Lane M, Thompson JG. Oocyte-secreted factors: regulators of cumulus cell function and oocyte quality. Hum Reprod Update. 2008 Mar-Apr;14(2):159-77.
19. Yamaguchi R, Perkins G. Dynamics of mitochondrial structure during apoptosis and the enigma of Opa1. Biochim Biophys Acta. 2009 Aug;1787(8):963-72.
20. Li CH, Cheng YW, Liao PL, Yang YT, Kang JJ. Chloramphenicol causes mitochondrial stress, decreases ATP biosynthesis, induces matrix metalloproteinase-13 expression, and solid-tumor cell invasion. Toxicol Sci. 2010 Jul;116(1):140-50.
21. Margolin W. FtsZ and the division of prokaryotic cells and organelles. Nat Rev Mol Cell Biol. 2005 Nov;6(11):862-71.
22. Zeth K, Thein M. Porins in prokaryotes and eukaryotes: common themes and variations. Biochem J. 2010 Oct 1;431(1):13-22.
23. Mileykovskaya E, Dowhan W. Cardiolipin membrane domains in prokaryotes and eukaryotes. Biochim Biophys Acta. 2009 Oct;1788(10):2084-91.
24. Passarella S, Atlante A, Valenti D, de Bari L. The role of mitochondrial transport in energy metabolism. Mitochondrion. 2003 Apr;2(5):319-43.
25. Battelli, F., and L. Stern. 1912. Ergeb. Physiol 15:96-268
26. Warburg, O. Arch. Gesamte. Physiol 1913. 154:599-617.
27. Warburg, O. Biochem. Z. 1926. 177:471-486.
28. Lehninger A.L., Nelson D., Cox M. Principles of Biochemistry. 2010.
29. Jackson JG, Thayer SA. Mitochondrial modulation of Ca2+ -induced Ca2+ -release in rat sensory neurons. J Neurophysiol. 2006 Sep;96(3):1093-104.
30. Liao Y, Dong Y, Cheng J. The Function of the Mitochondrial Calcium Uniporter in Neurodegenerative Disorders. Int J Mol Sci. 2017 Feb 10;18(2).
31. Annunziata I, d'Azzo A. Interorganellar membrane microdomains: dynamic platforms in the control of calcium signaling and apoptosis. Cells. 2013 Aug 2;2(3):574-90.
32. Vianello A, Casolo V, Petrussa E, Peresson C, Patui S, Bertolini A, Passamonti S, Braidot E, Zancani M. The mitochondrial permeability transition pore (PTP) - an example of multiple molecular exaptation? Biochim Biophys Acta. 2012 Nov;1817(11):2072-86.

33. Frank S, Gaume B, Bergmann-Leitner ES, Leitner WW, Robert EG, Catez F, Smith CL, and Youle RJ. The role of dynamin-related protein 1, a mediator of mitochondrial fission, in apoptosis. Dev. Cell, 2001. 1:515-525
34. Youle RJ, van der Bliek AM. Mitochondrial fission, fusion, and stress. Science. 2012 Aug 31;337(6098):1062-5.
35. Figueira TR, Barros MH, Camargo AA, Castilho RF, Ferreira JC, Kowaltowski AJ, Sluse FE, Souza-Pinto NC, Vercesi AE. Mitochondria as a source of reactive oxygen and nitrogen species: from molecular mechanisms to human health. Antioxid Redox Signal. 2013 Jun 1;18(16):2029-74.
36. Chen Q, Vazquez EJ, Moghaddas S, Hoppel CL, Lesnefsky EJ. Production of reactive oxygen species by mitochondria: central role of complex III. J Biol Chem. 2003 Sep 19;278(38):36027-31.
37. Birben E, Sahiner UM, Sackesen C, Erzurum S, Kalayci O. Oxidative stress and antioxidant defense. World Allergy Organ J. 2012 Jan;5(1):9-19.
38. Girotti AW. Lipid hydroperoxide generation, turnover, and effector action in biological systems. J Lipid Res. 1998 Aug;39(8):1529-42.
39. Genestra M. Oxyl radicals, redox-sensitive signalling cascades and antioxidants. Review Cell Signal. 2007;19(9):1807–1819.
40. Kohen R, Nyska A. Invited review Oxidation of Biological Systems: Oxidative Stress Phenomena, Antioxidants, Redox Reactions, and Methods for Their Quantification. Toxicol Pathol. 2002;30(6):620–650.
41. Sena LA, Chandel NS. Physiological roles of mitochondrial reactive oxygen species. Mol Cell. 2012 Oct 26;48(2):158-67
42. Murphy MP. How mitochondria produce reactive oxygen species. Biochem J. 2009 Jan 1;417(1):1-13.
43. Meister A. Mitochondrial changes associated with glutathione deficiency. Biochim Biophys Acta. 1995 May 24;1271(1):35-42.
44. Houtkooper RH, Vaz FM. Cardiolipin, the heart of mitochondrial metabolism. Cell Mol Life Sci. 2008 Aug;65(16):2493-506.
45. Fry M, Green DE. Cardiolipin requirement for electron transfer in complex I and III of the mitochondrial respiratory chain, J. Biol. Chem. 1981 Feb 25; 256 (4): 1874–80.
46. Paradies G, Petrosillo G, Pistolese M, Ruggiero FM. Reactive oxygen species affect mitochondrial electron transport complex I activity through oxidative cardiolipin damage. Gene. 2002 Mar 6;286(1): 135–41.

47. Dröse S, Zwicker K, Brandt U. Full recovery of the NADH:ubiquinone activity of complex I (NADH:ubiquinone oxidoreductase) from Yarrowia lipolytica by the addition of phospholipids. Biochim. Biophys. Acta 2002 Oct 3;1556 (1): 65–72.
48. Gomez Jr. B, Robinson NC. Phospholipase digestion of bound cardiolipin reversibly inactivates bovine cytochrome bc1. Biochemistry 1999 Jul 13; 38 (28): 9031–8.
49. Lange C, Nett JH, Trumpower BL, Hunte C. Specific roles of protein–phospholipid interactions in the yeast cytochrome bc1 complex structure. EMBO J. 2001 Dec 3; 20 (23): 6591–600.
50. Robinson NC. Functional binding of cardiolipin to cytochrome c oxidase. J. Bioenerg. Biomembr. 1993 Apr; 25(2): 153–63.
51. Eble KS, Coleman WB, Hantgan RR, Cunningham CC. Tightly associated cardiolipin in the bovine heart mitochondrial ATP synthase as analyzed by 31P nuclear magnetic resonance spectroscopy. J. Biol. Chem. 1990 Nov 15;265(32): 19434–40.
52. Ozawa T, Tanaka M, Wakabayashi T., Crystallization of mitochondrial cytochrome oxidase. Proc. Natl. Acad. Sci. U. S. A. 1982 Dec; 79(23) 7175–9.
53. Pebay-Peyroula E, Dahout-Gonzalez C, Kahn R, Trézéguet V, Lauquin GJ, Brandolin G. Structure of mitochondrial ADP/ATP carrier in complex with carboxyatractyloside. Nature 2003 Nov 6;426(6962): 39–44.
54. Claypool SM. Cardiolipin, a critical determinant of mitochondrial carrier protein assembly and function. Biochim Biophys Acta. 2009 Oct;1788(10):2059-68.
55. Imai H, Koumura T, Nakajima R, Nomura K, Nakagawa Y. Protection from inactivation of the adenine nucleotide translocator during hypoglycaemia-induced apoptosis by mitochondrial phospholipid hydroperoxide glutathione peroxidase. Biochem J. 2003 May 1;371(Pt 3):799-809.
56. Sedlák E, Robinson NC. Phospholipase A(2) digestion of cardiolipin bound to bovine cytochrome c oxidase alters both activity and quaternary structure, Biochemistry. 1999 Nov 9; 38 (45): 14966–72.
57. Gomez Jr. B, Robinson NC. Phospholipase digestion of bound cardiolipin reversibly inactivates bovine cytochrome bc1, Biochemistry 1999 Jul 13; 38 (28): 9031–8.
58. Kagan VE, Tyurin VA, Jiang J, Tyurina YY, Ritov VB, Amoscato AA, Osipov AN, Belikova NA, Kapralov AA, Kini V, Vlasova II, Zhao Q, Zou M, Di P, Svistunenko DA, Kurnikov IV, Borisenko GG. Cytochrome c acts as a cardiolipin

oxygenase required for release of proapoptotic factors. Nat Chem Biol. 2005 Sep;1(4):223-32.
59. Petrosillo G, Ruggiero FM, Pistolese M, Paradies G. Reactive oxygen species generated from the mitochondrial electron transport chain induce cytochrome c dissociation from beef-heart submitochondrial particles via cardiolipin peroxidation. Possible role in the apoptosis. FEBS Lett. 2001 Dec 14;509(3):435-8.
60. Petrosillo G, Casanova G, Matera M, Ruggiero FM, Paradies G. Interaction of peroxidized cardiolipin with rat-heart mitochondrial membranes: induction of permeability transition and cytochrome c release. FEBS Lett. 2006 Nov 27; 580 (27): 6311–6.
61. Petrosillo G, Moro N, Ruggiero FM, Paradies G. Melatonin inhibits cardiolipin peroxidation in mitochondria and prevents the mitochondrial permeability transition and cytochrome c release, Free Radic. Biol. Med. 2009 Oct 1; 47(7): 969–74.
62. Boveris A, Navarro A. Brain mitochondrial dysfunction in aging. IUBMB Life. 2008; 60:308–14.
63. Bertoni-Freddari C, Fattoretti P, Giorgetti B, Solazzi M, Balietti M, Meier-Ruge W. Role of mitochondrial deterioration in physiological and pathological brain aging. Gerontology. 2004 May-Jun;50(3):187-92.
64. Völgyi K, Gulyássy P, Háden K, Kis V, Badics K, Kékesi KA, Simor A, Györffy B, Tóth EA, Lubec G, Juhász G, Dobolyi A. Synaptic mitochondria: a brain mitochondria cluster with a specific proteome. J Proteomics. 2015 Apr 29;120:142-57.
65. Bertoni-Freddari C, Fattoretti P, Paoloni R, Caselli U, Meier-Ruge W. Impaired dynamic morphology of cerebellar mitochondria in physiological aging and Alzheimer's disease. Ann N Y Acad Sci. 1997 Sep 26;826:479-82.
66. Harman D. Aging: a theory based on free radical and radiation chemistry. J Gerontol. 1956 Jul;11(3):298-300.
67. Viña J, Sastre J, Pallardó F, Borrás C. Mitochondrial theory of aging: importance to explain why females live longer than males. Antioxid Redox Signal. 2003 Oct;5(5):549-56.
68. Gardner PR, Nguyen DD, White CW. Aconitase is a sensitive and critical target of oxygen poisoning in cultured mammalian cells and in rat lungs. Proc Natl Acad Sci USA. 1994;91:12248–12252.

69. Gokulrangan, G.,Zaidi, A.,Michaelis, M. L., and Schoneich, C. Proteomic analysis of protein nitration in rat cerebellum: effect of biological aging. J. Neurochem. 2007 Mar; 100(6): 1494–504.
70. Navarro A, Gomez C, López-Cepero JM, Boveris A. Beneficial effects of moderate exercise on mice aging: survival, behavior, oxidative stress, and mitochondrial electron transfer. Am J Physiol Regul Integr Comp Physiol. 2004 Mar;286(3):R505-11
71. Halliwell B. Reactive oxygen species and the central nervous system. J Neurochem. 1992 Nov;59(5):1609-23.
72. Chakrabarti S, Munshi S, Banerjee K, Thakurta IG, Sinha M, Bagh MB. Mitochondrial Dysfunction during Brain Aging: Role of Oxidative Stress and Modulation by Antioxidant Supplementation. Aging Dis. 2011 Jun;2(3):242-56.
73. Lesnefsky EJ, Hoppel CL. Oxidative phosphorylation and aging. Ageing Res Rev. 2006 Nov;5(4):402-33.
74. Guerrieri F, Capozza G,Kalous M, Zanotti F, Drahota Z, Papa S. Age-dependent changes in the mitochondrial F_OF_l ATP syntase. Arch Gerontol Geriat 1992; 14:299-308.
75. Davies SM, Poljak A, Duncan MW, Smythe GA, Murphy MP. Measurements of protein carbonyls, ortho- and meta-tyrosine and oxidative phosphorylation complex activity in mitochondria from young and old rats. Free Radic Biol Med 2001 Aug 15;31(4):559.
76. Ferrándiz ML, Martínez M, De Juan E, Díez A, Bustos G, Miquel J. Impairment of mitochondrial oxidative phosphorylation in the brain of aged mice. Brain Res. 1994 May 2;644(2):335-8.
77. Navarro A, Sánchez Del Pino MJ, Gómez C, Peralta JL, Boveris A. Behavioral dysfunction, brain oxidative stress, and impaired mitochondrial electron transfer in aging mice. Am J Physiol Regul Integr Comp Physiol. 2002 Apr;282(4):R985-92.
78. Corral-Debrinski M, Horton T, Lott MT, Shoffner JM, Beal MF, Wallace DC. Mitochondrial DNA deletions in human brain: regional variability and increase with advanced age. Nat Genet. 1992 Dec;2(4):324-9.
79. Lin MT, Simon DK, Ahn CH, Kim LM, Beal MF. High aggregate burden of somatic mtDNA point mutations in aging and Alzheimer's disease brain. Hum Mol Genet. 2002 Jan 15;11(2):133-45.
80. Soong NW, Hinton DR, Cortopassi G, Arnheim N. Mosaicism for a specific somatic mitochondrial DNA mutation in adult human brain. Nat Genet. 1992 Dec;2(4):318-23.

81. Baker BM, Haynes CM. Mitochondrial protein quality control during biogenesis and aging. Trends Biochem Sci. 2011 May;36(5):254-61.
82. Patergnani S, Pinton P. Mitophagy and mitochondrial balance. Methods Mol Biol. 2015;1241:181-94.
83. Geisler S, Holmstrom KM, Skujat D, Fiesel FC, Rothfuss OC, Kahle PJ, Springer W. PINK1/Parkin-mediated mitophagy is dependent on VDAC1 and p62/SQSTM1. Nat Cell Biol. 2010;12:119–131.
84. Matsuda N, Sato S, Shiba K, Okatsu K, Saisho K, Gautier CA, Sou YS, Saiki S, Kawajiri S, Sato F, et al. PINK1 stabilized by mitochondrial depolarization recruits Parkin to damaged mitochondria and activates latent Parkin for mitophagy. J Cell Biol. 2010;189:211–221.
85. Narendra D, Tanaka A, Suen DF, Youle RJ. Parkin is recruited selectively to impaired mitochondria and promotes their autophagy. J Cell Biol. 2008;183:795–803.
86. Pickrell AM, Youle RJ. The roles of PINK1, parkin, and mitochondrial fidelity in Parkinson's disease. Neuron. 2015 Jan 21;85(2):257-73.
87. Sun N, Yun J, Liu J, Malide D, Liu C, Rovira II, Holmström KM, Fergusson MM, Yoo YH, Combs CA, Finkel T. Measuring In Vivo Mitophagy. Mol Cell. 2015 Nov 19;60(4):685-96.
88. Exner N, Lutz AK, Haass C, Winklhofer KF. Mitochondrial dysfunction in Parkinson's disease: molecular mechanisms and pathophysiological consequences. EMBO J. 2012 Jun 26;31(14):3038-62.
89. Batlevi Y, La Spada AR. Mitochondrial autophagy in neural function, neurodegenerative disease, neuron cell death, and aging. Neurobiol Dis. 2011 Jul;43(1):46-51.
90. Yen WL, Klionsky DJ. How to live long and prosper: autophagy, mitochondria, and aging. Physiology (Bethesda). 2008 Oct;23:248-62.
91. Lee J, Giordano S, Zhang J. Autophagy, mitochondria and oxidative stress: cross-talk and redox signalling. Biochem J. 2012 Jan 15;441(2):523-40.
92. Kirkland RA, Adibhatla RM, Hatcher JF, Franklin JL. Loss of cardiolipin and mitochondria during programmed neuronal death: evidence of a role for lipid peroxidation and autophagy. Neuroscience. 2002;115(2):587-602.
93. Davalli P, Mitic T, Caporali A, Lauriola A, D'Arca D. ROS, Cell Senescence, and Novel Molecular Mechanisms in Aging and Age-Related Diseases. Oxid Med Cell Longev. 2016;2016:3565127.

94. Liu D, Xu Y. p53, oxidative stress, and aging. Antioxid Redox Signal. 2011 Sep 15;15(6):1669-78.
95. Lin MT, Beal MF. Mitochondrial dysfunction and oxidative stress in neurodegenerative diseases. Nature. 2006 Oct 19;443(7113):787-95.
96. McKhann G, Drachman D, Folstein M, Katzman R, Price D, Stadlan EM. Clinical diagnosis of Alzheimer's disease: report of the NINCDS-ADRDA Work Group under the auspices of Department of Health and Human Services Task Force on Alzheimer's Disease. Neurology. 1984 Jul;34(7):939-44.
97. Richens JL, Vere KA, Light RA, Soria D, Garibaldi J, Smith AD, Warden D, Wilcock G, Bajaj N, Morgan K, O'Shea P. Practical detection of a definitive biomarker panel for Alzheimer's disease; comparisons between matched plasma and cerebrospinal fluid. Int J Mol Epidemiol Genet. 2014 May 29;5(2):53-70.
98. Swerdlow RH, Burns JM, Khan SM. The Alzheimer's disease mitochondrial cascade hypothesis. J Alzheimers Dis. 2010;20 Suppl 2:S265-79.
99. Johri A, Beal MF. Mitochondrial dysfunction in neurodegenerative diseases. J Pharmacol Exp Ther. 2012 Sep;342(3):619-30.
100. Bubber P, Haroutunian V, Fisch G, Blass JP, Gibson GE. Mitochondrial abnormalities in Alzheimer brain: mechanistic implications. Ann Neurol. 2005 May;57(5):695-703.
101. Bosetti F, Brizzi F, Barogi S, Mancuso M, Siciliano G, Tendi EA, Murri L, Rapoport SI, Solaini G. Cytochrome c oxidase and mitochondrial F1F0-ATPase (ATP synthase) activities in platelets and brain from patients with Alzheimer's disease. Neurobiol Aging. 2002 May-Jun;23(3):371-6.
102. Sheng B, Wang X, Su B, Lee HG, Casadesus G, Perry G, Zhu X. Impaired mitochondrial biogenesis contributes to mitochondrial dysfunction in Alzheimer's disease. J Neurochem. 2012 Feb;120(3):419-29.
103. Hoehn MM, Yahr MD. Parkinsonism: onset, progression and mortality. Neurology. 1967 May;17(5):427-42.
104. Beitz JM. Parkinson's disease: a review. Front Biosci (Schol Ed). 2014 Jan 1;6:65-74.
105. Postuma RB, Gagnon JF, Montplaisir J. Clinical prediction of Parkinson's Disease: Planning for the age of neuroprotection. J Neurol Neurosurg Psychiatry. 2010 Sep; 81(9): 1008-13.
106. Alexander GE. Biology of Parkinson's disease: pathogenesis and pathophysiology of a multisystem neurodegenerative disorder. Dialogues Clin Neurosci. 2004 Sep;6(3):259-80.

107. Schapira AH, Cooper JM, Dexter D, Jenner P, Clark JB, Marsden CD. Mitochondrial complex I deficiency in Parkinson's disease. Lancet. 1989 Jun 3;1(8649):1269.
108. Parker WD Jr, Parks JK, Swerdlow RH. Complex I deficiency in Parkinson's disease frontal cortex. Brain Res. 2008 Jan 16;1189:215-8.
109. Bender A, Krishnan KJ, Morris CM, Taylor GA, Reeve AK, Perry RH, Jaros E, Hersheson JS, Betts J, Klopstock T, Taylor RW, Turnbull DM. High levels of mitochondrial DNA deletions in substantia nigra neurons in aging and Parkinson disease. Nat Genet. 2006 May;38(5):515-7.
110. Hirst J, King MS, Pryde KR. The production of reactive oxygen species by complex I. Biochem Soc Trans. 2008 Oct;36(Pt 5):976-80.
111. Kitada T, Asakawa S, Hattori N, Matsumine H, Yamamura Y, Minoshima S, Yokochi M, Mizuno Y and Shimizu N. Mutations in the parkin gene cause autosomal recessive juvenile parkinsonism. Nature. 1998 Apr 9; 392 (6676), 605–8.
112. Valente EM, Abou-Sleiman PM, Caputo V, Muqit MM, Harvey K, Gispert S, Ali Z, Del Turco D, Bentivoglio AR, Healy DG, Albanese A, Nussbaum R, González-Maldonado R, Deller T, Salvi S, Cortelli P, Gilks WP, Latchman DS, Harvey RJ, Dallapiccola B, Auburger G, Wood NW. Hereditary early-onset Parkinson's disease caused by mutations in PINK1. Science. 2004 May 21;304(5674):1158-60.
113. Bonifati V, Rizzu P, van Baren MJ, Schaap O, Breedveld GJ, Krieger E, Dekker MC, Squitieri F, Ibanez P, Joosse M, van Dongen JW, Vanacore N, van Swieten JC, Brice A, Meco G, van Duijn CM, Oostra BA, Heutink P. Mutations in the DJ-1 gene associated with autosomal recessive early-onset parkinsonism. Science. 2003 Jan 10;299(5604):256-9.
114. Taira T, Saito Y, Niki T, Iguchi-Ariga SM, Takahashi K, Ariga H. DJ-1 has a role in antioxidative stress to prevent cell death. EMBO Rep. 2004 Feb;5(2):213-8.
115. McCoy MK, Cookson MR. DJ-1 regulation of mitochondrial function and autophagy through oxidative stress. Autophagy. 2011 May;7(5):531-2.
116. Irrcher I, Aleyasin H, Seifert EL, Hewitt SJ, Chhabra S, Phillips M, Lutz AK, Rousseaux MW, Bevilacqua L, Jahani-Asl A, Callaghan S, MacLaurin JG, Winklhofer KF, Rizzu P, Rippstein P, Kim RH, Chen CX, Fon EA, Slack RS, Harper ME, McBride HM, Mak TW, Park DS. Loss of the Parkinson's disease-linked gene DJ-1 perturbs mitochondrial dynamics. Hum Mol Genet. 2010 Oct 1;19(19):3734-46.

117. Gandhi PN, Chen SG, Wilson-Delfosse AL. Leucine-rich repeat kinase 2 (LRRK2): a key player in the pathogenesis of Parkinson's disease. J Neurosci Res. 2009 May 1;87(6):1283-95.
118. West AB, Moore DJ, Biskup S, Bugayenko A, Smith WW, Ross CA, Dawson VL, Dawson TM. Parkinson's disease-associated mutations in leucine-rich repeat kinase 2 augment kinase activity. Proc Natl Acad Sci U S A. 2005 Nov 15;102(46):16842-7.
119. Woods AS, Jackson SN. Brain tissue lipidomics: direct probing using matrix-assisted laser desorption/ionization mass spectrometry. AAPS J. 2006 Jun 2;8(2):E391-5.
120. O'Brien JS, Sampson EL. Lipid composition of the normal human brain: gray matter, white matter, and myelin. J Lipid Res. 1965 Oct;6(4):537-44.
121. Veloso A, Fernández R, Astigarraga E, Barreda-Gómez G, Manuel I, Giralt MT, Ferrer I, Ochoa B, Rodríguez-Puertas R, Fernández JA. Distribution of lipids in human brain. Anal Bioanal Chem. 2011 Jul;401(1):89-101.
122. Farooqui AA, Horrocks LA, Farooqui T. Glycerophospholipids in brain: their metabolism, incorporation into membranes, functions, and involvement in neurological disorders. Chem Phys Lipids. 2000 Jun;106(1):1-29.
123. Van Meer G. Lipid traffic in animal cells. Annu Rev Cell Biol. 1989;5:247-75.
124. Cantù L, Del Favero E, Sonnino S, Prinetti A. Gangliosides and the multiscale modulation of membrane structure. Chem Phys Lipids. 2011 Nov;164(8):796-810.
125. Krafft C, Neudert L, Simat T, Salzer R. Near infrared Raman spectra of human brain lipids. Spectrochim Acta A Mol Biomol Spectrosc. 2005 May;61(7):1529-35.
126. Sonnino S, Chigorno V. Ganglioside molecular species containing C18- and C20-sphingosine in mammalian nervous tissues and neuronal cell cultures. Biochim Biophys Acta. 2000 Sep 18;1469(2):63-77.
127. Sonnino S, Mauri L, Chigorno V, Prinetti A. Gangliosides as components of lipid membrane domains. Glycobiology. 2007 Jan;17(1):1R-13R.
128. Svennerholm L. Chromatographic separation of human brain gangliosides. J. Neurochem. 1963 Sep;10:613-23.
129. Svennerholm L. The gangliosides. J Lipid Res. 1964 Apr;5:145-55.
130. Benjamins Ja, Hajira AK, Agranoff BW. Chapter 3 Lipids. In Brady, Scott T., George J. Siegel, R. Wayne. Albers, and Donald L. Price. Basic Neurochemistry Molecular, Cellular, and Medical Aspects. Amsterdam: Academic, 2012 pag. 33-48

131. Crews, FT. Rapid changes in phospholipid metabolism during secretion and receptor activation. Int Rev Neurobiol. 1982;23: 141-63.
132. Freysz L, Dreyfus H, Vincendon G, Binaglia L, Roberti R, Porcellati G, 1982. Asymmetry of brain microsomal membranes: correlation between the asymmetric distribution of phospholipids and the enzymes involved in their synthesis. In: Horrocks, L.A., Ansell, G.B., Porcellati, G. (Eds.), Phospholipids in the Nervous System. Raven Press, New York, pp. 37-47.
133. Dennis EA, Rhee SG, Billah MM, Hannun YA. Role of phospholipase in generating lipid second messengers in signal transduction. FASEB J. 1991 Apr;5(7):2068-77.
134. Kornecki E, Wieraszko A, Chan JC, Ehrlich YH. Platelet activating factor (PAF) in memory formation: role as a retrograde messenger in long-term potentiation. J. Lipid Mediat Cell Signal. 1996 Sep;14 (1-3): 115-126.
135. Feuerstein GZ. Platelet-activating factor: a case for its role in CNS function and brain injury. J Lipid Mediat Cell Signal. 1996 Sep;14(1-3):109-14.
136. Panganamala RV, Horrocks LA, Geer JC, Cornwell DG. Positions of double bonds in the monounsaturated alk-1-enyl groups from the plasmalogens of human heart and brain. Chem Phys Lipids. 1971 May;6(2):97-102.
137. Brosche T. Plasmalogen phospholipids - facts and theses to their antioxidative qualities. Arch Gerontol Geriatr. 1997 Jul-Aug;25(1):73-81.
138. Lohner K. Is the high propensity of ethanolamine plasmalogens to form non-lamellar lipid structures manifested in the properties of biomembranes? Chem Phys Lipids. 1996 Jul 15;81(2):167-84.
139. Aureli M., Loberto N., Lanteri P., Chigorno V., Prinetti A. and Sonnino S. Cell surface sphingolipid glycohydrolases in neuronal differentiation and aging in culture. J. Neurochem. 2011 Mar;116 (5): 891–9.
140. Pettus BJ, Chalfant CE, Hannun YA. Ceramide in apoptosis: an overview and current perspectives. Biochim Biophys Acta. 2002 Dec 30;1585(2-3):114-25.
141. Hannun YA, Obeid LM: Principles of bioactive lipid signalling: Lessons from sphingolipids. Nat Rev Mol Cell Biol 2008;9:139-150.
142. Mizugishi K, Yamashita T, Olivera A, Miller GF, Spiegel S, Proia RL: Essential role for sphingosine kinases in neural and vascular development. Mol Cell Biol 2005;25:11113-11121.
143. Meyer zu Heringdorf D, Liliom K, Schaefer M, Danneberg K, Jaggar JH, Tigyi G, Jakobs KH: Photolysis of intracellular caged sphingosine-1-phosphate causes

Ca2+ mobilization independently of G-protein-coupled receptors. FEBS Lett 2003;554:443-449.
144. Olivera A, Spiegel S: Sphingosine-1-phosphate as second messenger in cell proliferation induced by PDGF and FCS mitogens. Nature 1993;365:557-560.
145. Cuvillier O, Pirianov G, Kleuser B, Vanek PG, Coso OA, Gutkind S, Spiegel S: Suppression of ceramide-mediated programmed cell death by sphingosine-1-phosphate. Nature 1996;381:800-803.
146. Olivera A, Rosenfeldt HM, Bektas M, Wang F, Ishii I, Chun J, Milstien S, Spiegel S: Sphingosine kinase type 1 induces G12/13-mediated stress fiber formation, yet promotes growth and survival independent of G protein-coupled receptors. J Biol Chem 2003;278:46452-46460.
147. Hait NC, Allegood J, Maceyka M, Strub GM, Harikumar KB, Singh SK, Luo C, Marmorstein R, Kordula T, Milstien S, Spiegel S: Regulation of histone acetylation in the nucleus by sphingosine-1-phosphate. Science 2009;325:1254-1257.
148. Bagdanoff JT, Donoviel MS, Nouraldeen A, Tarver J, Fu Q, Carlsen M, Jessop TC, Zhang H, Hazelwood J, Nguyen H, Baugh SD, Gardyan M, Terranova KM, Barbosa J, Yan J, Bednarz M, Layek S, Courtney LF, Taylor J, Digeorge-Foushee AM, Gopinathan S, Bruce D, Smith T, Moran L, O'Neill E, Kramer J, Lai Z, Kimball SD, Liu Q, Sun W, Yu S, Swaffield J, Wilson A, Main A, Carson KG, Oravecz T, Augeri DJ: Inhibition of sphingosine-1-phosphate lyase for the treatment of autoimmune disorders. J Med Chem 2009;52:3941-3953.
149. Colombaioni L, Garcia-Gil M. Sphingolipid metabolites in neural signalling and function. Brain Res Brain Res Rev. 2004 Nov;46(3):328-55.
150. Arana L, Gangoiti P, Ouro A, Trueba M, Gómez-Muñoz A. Ceramide and ceramide 1-phosphate in health and disease. Lipids Health Dis. 2010 Feb 5;9:15.
151. Pike LJ. Lipid rafts: bringing order to chaos. J Lipid Res. 2003 Apr;44(4):655-67.
152. Maccarrone M, Bernardi G, Agrò AF, Centonze D. Cannabinoid receptor signalling in neurodegenerative diseases: a potential role for membrane fluidity disturbance. Br J Pharmacol. 2011 Aug;163(7):1379-90.
153. Sebastiao AM, Assaife-Lopes N, Diogenes MJ, Vaz SH, Ribeiro JA (2011) Modulation of brain-derived neurotrophic factor (BDNF) actions in the nervous system by adenosine A(2A) receptors and the role of lipid rafts. Biochim Biophys Acta 1808:1340–1349
154. D'Ambrosi N, Volonte C. Metabotropic purinergic receptors in lipid membrane microdomains. Curr Med Chem. 2013;20(1):56–63

155. Sonnino S, Aureli M, Grassi S, Mauri L, Prioni S, Prinetti A. Lipid rafts in neurodegeneration and neuroprotection. Mol Neurobiol. 2014 Aug;50(1):130-48.
156. Fantini J, Barrantes FJ. Sphingolipid/cholesterol regulation of neurotransmitter receptor conformation and function. Biochim Biophys Acta. 2009 Nov;1788(11):2345-61.
157. Yeagle PL. Modulation of membrane function by cholesterol. Biochimie. 1991 Oct;73(10):1303-10.
158. Goedeke L, Fernández-Hernando C. MicroRNAs: a connection between cholesterol metabolism and neurodegeneration. Neurobiol Dis. 2014 Dec;72 Pt A:48-53.
159. Kim J, Yoon H, Ramírez CM, Lee SM, Hoe HS, Fernández-Hernando C, Kim J. MiR-106b impairs cholesterol efflux and increases Aβ levels by repressing ABCA1 expression. Exp Neurol. 2012 Jun;235(2):476-83.
160. Slotte JP. Biological functions of sphingomyelins. Prog Lipid Res. 2013 Oct;52(4):424-37.
161. Hakomori S, Handa K, Iwabuchi K, Yamamura S, Prinetti A. New insights in glycosphingolipid function: "glycosignaling domain," a cell surface assembly of glycosphingolipids with signal transducer molecules, involved in cell adhesion coupled with signaling. Glycobiology. 1998 Oct;8(10):xi-xix.
162. Ledeen RW, Wu G. Nuclear sphingolipids: metabolism and signaling. J Lipid Res. 2008 Jun;49(6):1176-86.
163. Yu RK, Tsai YT, Ariga T, Yanagisawa M. Structures, biosynthesis, and functions of gangliosides-an overview. J Oleo Sci. 2011;60(10):537-44.
164. Vinson M, Strijbos PJ, Rowles A, Facci L, Moore SE, Simmons DL, Walsh FS. Myelin-associated glycoprotein interacts with ganglioside GT1b. A mechanism for neurite outgrowth inhibition. J Biol Chem. 2001 Jun 8;276(23):20280-5.
165. Dowhan W. Molecular basis for membrane phospholipid diversity: why are there so many lipids? Annu Rev Biochem. 1997;66:199-232.
166. Daum G. Lipids of mitochondria. Biochim Biophys Acta. 1985; 822:1–42.
167. Campbell AM, Chan SH. Mitochondrial membrane cholesterol, the voltage dependent anion channel (VDAC), and the Warburg effect. J Bioenerg Biomembr. 2008
168. Becker T, Horvath SE, Böttinger L, Gebert N, Daum G, Pfanner N. Role of phosphatidylethanolamine in the biogenesis of mitochondrial outer membrane proteins. J Biol Chem. 2013 Jun 7;288(23):16451-9.

169. Kiebish MA, Han X, Seyfried TN. Examination of the brain mitochondrial lipidome using shotgun lipidomics. Methods Mol Biol. 2009;579:3-18.
170. Claude A. Particulate components of normal and tumor cells. Science. 1940 Jan 19;91(2351):77-8.
171. Bensley RR, Hoerr N. Studies on cell structure by the freezing-drying method. VI. The preparation and properties of mitochondria. Anat. Record. 1934 60; 499-455.
172. Claude A. Fractionation of mammalian liver cells by differential centrifugation; experimental procedures and results. J Exp Med. 1946 Jul;84:61-89.
173. Claude A. The constitution of mitochondria and microsomes, and the distribution of nucleic acid in the cytoplasm of leukemic cell. J Exp Med. 1944 Jul 1;80(1):19-29.
174. Hogeboom GH, Schneider WC, Pallade GE. The isolation of morphologically intact mitochondria from rat liver. Proc Soc Exp Biol Med. 1947 Jun;65(2):320.
175. Schneider WC, Hogeboom GH. Intracellular distribution of enzymes. V. Further studies on the distribution of cytochrome c in rat liver homogenates. J Biol. Chem. 1950 183:123-128.
176. Lai JCK, Walsh JM, Dennis SC, Clark JB. Synaptic and non-synaptic mitochondria from rat-brain—isolation and characterization. Journal of Neurochemistry 1977;28:625–31.
177. Sims NR. Rapid isolation of metabolically active mitochondria from rat-brain and subregions using Percoll density gradient centrifugation. Journal of Neurochemistry 1990;55:698–707.
178. Anderson MF, Sims NR. Improved recovery of highly enriched mitochondrial fractions from small brain tissue samples. Brain Research Protocols 2000;5:95–101.
179. Brown MR, Sullivan PG, Dorenbos KA, Modafferi EA, Geddes JW, Steward O. Nitrogen disruption of synaptoneurosomes: an alternative method to isolate brain mitochondria. J Neurosci Methods. 2004 Aug 30;137(2):299-303.
180. Sims NR, Anderson MF. Isolation of mitochondria from rat brain using Percoll density gradient centrifugation. Nature Protocols 2008;3:1228–38.
181. Barksdale KA, Perez-Costas E, Gandy JC, Melendez-Ferro M, Roberts RC, Bijur GN. Mitochondrial viability in mouse and human post mortem brain. FASEB J. 2010 Sep;24(9):3590-3599.
182. Kristian T. Isolation of mitochondria from the CNS. Curr Protoc Neurosci. 2010 Jul;Chapter 7:Unit 7.22.

183. Chinopoulos C, Zhang SF, Thomas B, Ten V, Starkov AA. Isolation and functional assessment of mitochondria from small amounts of mouse brain tissue. Methods Mol Biol. 2011;793:311-324.
184. Iglesias-González J, Sánchez-Iglesias S, Beiras-Iglesias A, Soto-Otero R, Méndez-Álvarez E. A simple method for isolating rat brain mitochondria with high metabolic activity: effects of EDTA and EGTA. J Neurosci Methods. 2013 Feb 15;213(1):39-42.
185. Fang X, Wang W, Yang L, Chandrasekaran K, Kristian T, Balgley BM, Lee CS. Application of capillary isotachophoresis-based multidimensional separations coupled with electrospray ionization-tandem mass spectrometry for characterization of mouse brain mitochondrial proteome. Electrophoresis. 2008 May;29(10):2215-23.
186. Fang X, Lee CS. Proteome characterization of mouse brain mitochondria using electrospray ionization tandem mass spectrometry. Methods Enzymol. 2009;457:49-62.
187. Franko A, Baris OR, Bergschneider E, von Toerne C, Hauck SM, Aichler M, Walch AK, Wurst W, Wiesner RJ, Johnston IC, de Angelis MH. Efficient isolation of pure and functional mitochondria from mouse tissues using automated tissue disruption and enrichment with anti-TOM22 magnetic beads. PLoS One. 2013 Dec 12;8(12):e82392.
188. Khattar NK, Yablonska S, Baranov SV, Baranova OV, Kretz ES, Larkin TM, Carlisle DL, Richardson RM, Friedlander RM. Isolation of functionally active and highly purified neuronal mitochondria from human cortex. J Neurosci Methods. 2016 Jan 22;263:1-6. doi: 10.1016/j.jneumeth.2016.01.017.
189. Morgunov I, Srere PA. Interaction between citrate synthase and malate dehydrogenase. Substrate channeling of oxaloacetate. J Biol Chem. 1998 Nov 6;273(45):29540-4.
190. Lowry OH, Rosebrough NJ, Farr AL, Randall RJ. Protein measurement with the Folin phenol reagent. J Biol Chem. 1951 Nov;193(1):265-75.
191. Laemmli UK. Cleavage of structural proteins during the assembly of the head of bacteriophage T4. Nature. 1970 Aug 15;227(5259):680-5.
192. Scandroglio, F., N. Loberto, M. Valsecchi, V. Chigorno, A. Prinetti, and S. Sonnino, (2009), Glycoconj. J. 26(8), 961-73.
193. Pollard AK, Ortori CA, Stöger R, Barrett DA, Chakrabarti L. Mouse mitochondrial lipid composition is defined by age in brain and muscle. Aging (Albany NY). 2017 Mar 21;9(3):986-998.

194. Modi HR, Katyare SS, Patel MA. Ageing-induced alterations in lipid/phospholipid profiles of rat brain and liver mitochondria: implications for mitochondrial energy-linked functions. J Membr Biol. 2008 Jan;221(1):51-60.
195. Toescu EC, Myronova N, Verkhratsky A. Age-related structural and functional changes of brain mitochondria. Cell Calcium. 2000 Nov-Dec;28(5-6):329-38.
196. Leighton F, Poole B, Beaufay H, Baudhuin P, Coffey JW, Fowler S, De Duve C. The large-scale separation of peroxisomes, mitochondria, and lysosomes from the livers of rats injected with triton WR-1339. Improved isolation procedures, automated analysis, biochemical and morphological properties of fractions. J Cell Biol. 1968 May;37(2):482-513.
197. Almeida A, Medina JM. A rapid method for the isolation of metabolically active mitochondria from rat neurons and astrocytes in primary culture. Brain Res Brain Res Protoc. 1998 Mar;2(3):209-14.
198. Lisman JJ, de Haan J, Overdijk B. Isolation of lysosomes from brain tissue. A separation method by means of alteration of mitochondrial and synaptosomal sedimentation properties. Biochem J. 1979 Jan 15;178(1):79-87.
199. Kovacs WJ, Faust PL, Keller GA, Krisans SK. Purification of brain peroxisomes and localization of 3-hydroxy-3-methylglutaryl coenzyme A reductase. Eur J Biochem. 2001 Sep;268(18):4850-9.
200. Szabadkai G, Bianchi K, Várnai P, De Stefani D, Wieckowski MR, Cavagna D, Nagy AI, Balla T, Rizzuto R. Chaperone-mediated coupling of endoplasmic reticulum and mitochondrial Ca2+ channels. J Cell Biol. 2006 Dec 18;175(6):901-11.
201. Horvath SE, Daum G. Lipids of mitochondria. Prog Lipid Res. 2013 Oct;52(4):590-614.
202. Matyas GR, Morré DJ. Subcellular distribution and biosynthesis of rat liver gangliosides. Biochim Biophys Acta. 1987 Oct 17;921(3):599-614.
203. Gillard BK, Thurmon LT, Marcus DM. Variable subcellular localization of glycosphingolipids. Glycobiology. 1993 Feb;3(1):57-67.
204. Scandroglio F, Venkata JK, Loberto N, Prioni S, Schuchman EH, Chigorno V, Prinetti A, Sonnino S. Lipid content of brain, brain membrane lipid domains, and neurons from acid sphingomyelinase deficient mice. J Neurochem. 2008 Oct;107(2):329-38.
205. Hsu P, Shi Y. Regulation of autophagy by mitochondrial phospholipids in health and diseases. Biochim Biophys Acta. 2017 Jan;1862(1):114-129.

206. Demel RA, De Kruyff B. The function of sterols in membranes. Biochim Biophys Acta. 1976 Oct 26;457(2):109-32.
207. Söderberg M, Edlund C, Kristensson K, Dallner G. Lipid compositions of different regions of the human brain during aging. J Neurochem. 1990 Feb;54(2):415-23.
208. Ruggiero FM, Cafagna F, Petruzzella V, Gadaleta MN, Quagliariello E. Lipid composition in synaptic and nonsynaptic mitochondria from rat brains and effect of aging. J Neurochem. 1992 Aug;59(2):487-91.
209. Segler-Stahl K, Webster JC, Brunngraber EG. Changes in the concentration and composition of human brain gangliosides with aging. Gerontology. 1983;29(3):161-8.
210. Morrison JH, Hof PR. Life and death of neurons in the aging brain. Science. 1997 Oct 17;278(5337):412-9.

8. Scientific productions

Publication:

- Moncini S, Lunghi M, Valmadre A, Grasso M, Del Vescovo V, Riva P, Denti MA, Venturin M. *The miR-15/107 Family of microRNA Genes Regulates CDK5R1/p35 with Implications for Alzheimer's Disease Pathogenesis*. Mol Neurobiol, 2016 Jun 24.

Poster presentation:

- Valmadre A, Prioni S, Zucca FA, Cabitta L, Prinetti A, Zecca L. *Lipid composition of human grey matter mitochondria in aging*. VIII World Congress on Targeting Mitochondria

9. Acknowledgments

Nel concludere questa terza (e forse ultima) tesi, desidero ringraziare tutte le persone che hanno reso possibile il raggiungimento di questo obiettivo. Innanzitutto desidero ringraziare la Prof.ssa Stefania Corti, sempre disponibile nei miei confronti, e il Dott. Luigi Zecca, per avermi permesso di svolgere questa appassionante attività di ricerca nel suo laboratorio.

Vorrei inoltre esprimere la mia più sincera gratitudine a Fabio per i suoi numerosi consigli, il suo costante supporto e la battuta sempre pronta a sdrammatizzare; a Chiara per essere stata un instancabile faro luminoso in questi anni, nonché una fantastica amica a tutti gli effetti; agli ex-membri del laboratorio Francesca, Emanuele e Ksenjia. Avete tutti contribuito fortemente alla mia crescita personale.

Desidero ringraziare di cuore anche il Prof. Alessandro Prinetti e Simona, per avermi guidata con estrema dedizione lungo il pezzetto di strada più impegnativo, ovvero l'ultimo. Grazie anche alle ragazze del loro laboratorio, soprattutto a Sara e Livia, senza le quali non avrei imparato a fare delle piccole opere d'arte con le lastre di TLC! Vi ringrazio tutti per avermi fatto sentire come se avessi sempre fatto parte del laboratorio.

Ringrazio vivamente anche la Dott.ssa Maria Carla Panzeri (Alembic – San Raffaele) per le fondamentali immagini di microscopia elettronica, e l'Istituto Di Medicina Legale E Delle Assicurazioni (Dipartimento di Scienze Biomediche per la Salute) per la collaborazione al reperimento di tessuti umani, risorse estremamente preziose e basilari per il mio lavoro di tesi.

Grazie anche ai miei "dirimpettai" di laboratorio, Nithiya, Federica, Aleksandra e Fulvio per le risate fatte insieme, che sollevano lo spirito e danno coraggio lungo il cammino.

Come potrei non ringraziare tutti i miei meravigliosi amici? Ilaria F., Simona, Maura, Letizia, Nicole, Ilaria B., Davide W., Eugenio, Alessio, Marco, Diana,

Cekko, Betty e Davide F., Saimon, Chiara, Giulio, Oscar, Luca e Davide C. Tutti insieme avete rappresentato una magnifica isola felice durante questo periodo.

Provo infinita gratitudine per il Prof. Antonio Nogara, che è entrato a far parte della mia famiglia come membro onorario e dal quale ho ricevuto costante incoraggiamento durante tutto il mio percorso di dottorato. Riconoscenza e affetto alle mie zie Laura ed Elena, che mi hanno formata fin da piccola, senza le quali non sarei arrivata dove sono oggi.

Infine, ma non per ultimi, i miei genitori e mio fratello, ai quali devo il ringraziamento più sentito, per essere stati ancora una volta i miei migliori alleati, la mia ancora, il sostegno più solido e sicuro che io possa trovare. Grazie dal più profondo del mio cuore anche ai miei nonni, siete e sarete sempre il vento che soffia a prua, che mi conduce verso i traguardi nell'oceano della vita.